



The potential of multispectral imaging flow cytometry for environmental monitoring

Susanne Dunker^{1,2}  | Matthew Boyd³ | Walter Durka^{4,2}  | Silvio Erler⁵  |
 W. Stanley Harpole^{1,2,6}  | Silvia Henning⁷  | Ulrike Herzschuh^{8,9,10}  |
 Thomas Hornick^{1,2}  | Tiffany Knight^{2,4,6}  | Stefan Lips¹¹  |
 Patrick Mäder^{2,12,13} | Elena Motivans Švara^{2,4,6}  | Steven Mozarowski³ |
 Demetra Rakosy^{2,4}  | Christine Römermann^{2,14}  | Mechthild Schmitt-Jansen¹¹  |
 Kathleen Stoof-Leichsenring⁸  | Frank Stratmann⁷  | Regina Treudler¹⁵  |
 Risto Virtanen¹⁶  | Katrin Wendt-Potthoff¹⁷  | Christian Wilhelm¹⁸

¹Department of Physiological Diversity, Helmholtz-Centre for Environmental Research (UFZ), Leipzig, Germany

²German Centre for Integrative Biodiversity Research (iDiv) Halle-Jena-Leipzig, Leipzig, Germany

³Department of Anthropology, Lakehead University, Thunder Bay, Canada

⁴Department of Community Ecology, Helmholtz-Centre for Environmental Research (UFZ), Halle, Germany

⁵Institute for Bee Protection, Julius Kühn Institute (JKI)-Federal Research Centre for Cultivated Plants, Braunschweig, Germany

⁶Institute of Biology, Martin Luther University Halle-Wittenberg, Halle, Germany

⁷Department of Experimental Aerosol and Cloud Microphysics, Leibniz Institute for Tropospheric Research (TROPOS), Leipzig, Germany

⁸Alfred-Wegener-Institute Helmholtz Centre of Polar and Marine Research, Polar Terrestrial Environmental Systems, Potsdam, Germany

⁹Institute of Environmental Sciences and Geography, University of Potsdam, Potsdam, Germany

¹⁰Institute of Biochemistry and Biology, University of Potsdam, Potsdam, Germany

¹¹Department of Bioanalytical Ecotoxicology, Helmholtz-Centre for Environmental Research – UFZ, Leipzig, Germany

¹²Department of Computer Science and Automation, Technische Universität Ilmenau, Ilmenau, Germany

Abstract

Environmental monitoring involves the quantification of microscopic cells and particles such as algae, plant cells, pollen, or fungal spores. Traditional methods using conventional microscopy require expert knowledge, are time-intensive and not well-suited for automated high throughput. Multispectral imaging flow cytometry (MIFC) allows measurement of up to 5000 particles per second from a fluid suspension and can simultaneously capture up to 12 images of every single particle for brightfield and different spectral ranges, with up to 60x magnification. The high throughput of MIFC has high potential for increasing the amount and accuracy of environmental monitoring, such as for plant-pollinator interactions, fossil samples, air, water or food quality that currently rely on manual microscopic methods. Automated recognition of particles and cells is also possible, when MIFC is combined with deep-learning computational techniques. Furthermore, various fluorescence dyes can be used to stain specific parts of the cell to highlight physiological and chemical features including: vitality of pollen or algae, allergen content of individual pollen, surface chemical composition (carbohydrate coating) of cells, DNA- or enzyme-activity staining. Here, we outline the great potential for MIFC in environmental research for a variety of research fields and focal organisms. In addition, we provide best practice recommendations.

KEYWORDS

environmental monitoring, imaging flow cytometry, plant traits

This is an open access article under the terms of the [Creative Commons Attribution-NonCommercial](https://creativecommons.org/licenses/by-nc/4.0/) License, which permits use, distribution and reproduction in any medium, provided the original work is properly cited and is not used for commercial purposes.

© 2022 The Authors. *Cytometry Part A* published by Wiley Periodicals LLC on behalf of International Society for Advancement of Cytometry.

¹³Faculty of Biological Sciences, Friedrich-Schiller-University Jena, Jena, Germany

¹⁴Institute of Ecology and Evolution, Friedrich-Schiller-University Jena, Jena, Germany

¹⁵Department of Dermatology, Venerology and Allergology, University of Leipzig Medical Center, Leipzig, Germany

¹⁶Ecology and Genetics, University of Oulu, Oulu, Finland

¹⁷Department of Lake Research, Helmholtz-Centre for Environmental Research – UFZ, Magdeburg, Germany

¹⁸Faculty of Life Sciences, Institute of Biology, University of Leipzig, Leipzig, Germany

Correspondence

Susanne Dunker, Department of Physiological Diversity, Helmholtz-Centre for Environmental Research (UFZ), Permoserstraße 15, 04318 Leipzig, Germany and German Centre for Integrative Biodiversity Research (iDiv) Halle-Jena-Leipzig, Leipzig, Germany.
 Email: susanne.dunker@ufz.de

Funding information

Bundesministerium für Bildung und Forschung, Grant/Award Number: 02WPL1448A; Bundesministerium für Ernährung und Landwirtschaft, Grant/Award Numbers: 2819NA066, 2819NA102, 2819NA106; Deutsche Forschungsgemeinschaft, Grant/Award Numbers: 34600830-13, 34600865-16, RA-373/20

1 | INTRODUCTION

Addressing many of our pressing environmental problems, such as air pollution by particulate matter, loss of pollinating insects, reduction of freshwater quality, contamination of food by microplastic particles or infection of crop plants by phytopathogenic fungi, require microscopic monitoring of small particles like particulate matter, microplastics, cells including cyanobacteria, algae, spores, pollen or organelles at sub-cellular level (Figure 1), which by the nature of their small sizes can be quite challenging. Microscopic environmental monitoring has relevance for several ecosystem services that impact our daily life, but also to better understand past life on earth. Basically, we need to know what species of microorganisms and types of particles are/were in the environment, in which abundance and which are of health, economic and ecological concerns. Some of these applications include environmental monitoring for air, food and water quality assessment, paleobotany, meteorology, microplastic contamination, ecological research or agriculture. In most of these monitoring tasks, microscopic species identification and quantification is crucial for environmental quality assessment. The traditional manual microscopic approach is time-intensive, requires expert-training and is not well-suited to automation or large sample numbers and thus limits the throughput to relatively few measurements. Although more and more alternative monitoring methods, such as metabarcoding, are emerging, traditional

microscopic monitoring is still the gold standard in most of the application fields (e.g., water quality monitoring or palynology). But fewer measurements means fewer locations or time points for monitoring and thus lower resolution of emerging potential environmental problems. Microscopic methods may be also prone to errors due to the subjectivity of the taxonomist or suboptimal slide conditions (e.g., high densities of cells obscuring each other), resulting in inaccurately differentiation. The switch to alternative methods, such as metabarcoding, is problematic, since decades-old time series of species/particle numbers can then no longer be adequately compared with current measurement data based on operational taxonomic units (OTU) or DNA sequence reads. Thus, molecular biological monitoring methods show only limited agreement with microscopic methods, especially with regard to the quantitative detection of particles [1, 2]. Imaging flow cytometry in combination with deep-learning computational techniques might overcome these limitations.

Originally developed for medical applications, multispectral imaging flow cytometry (MIFC) has the potential to make advancements in several microscopic tasks [3]. Due to key advantages over other identification methods. First, it allows cells and particles to be detected predominantly as individual objects due to hydrodynamic forcing and subsequent physical separation. Secondly, imaging flow cytometry combines flow cytometry with digital microscopy of every object and therefore provides quantitative high-throughput image data [4–6],

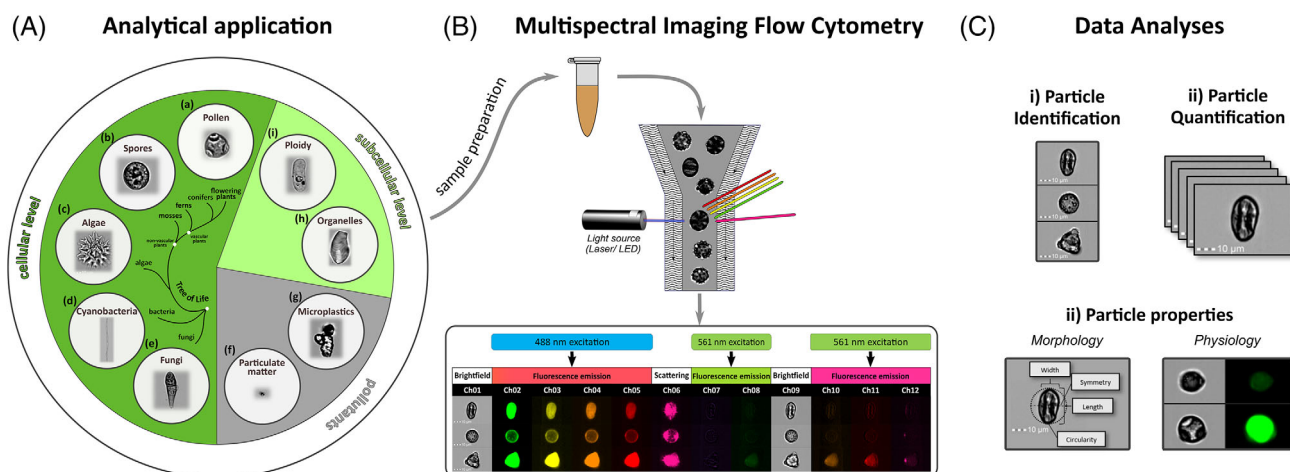


FIGURE 1 Overview about potential application fields of multispectral imaging flow cytometry and possible data output for environmental monitoring. Different particles are presented here as being relevant for environmental monitoring, for example (A) Pollen for air quality, plant-pollinator interactions (ecology, agriculture, food production) or paleoecology, (B) bryophyte spores for ecological research and as bio-indicators, (C) algae and (D) cyanobacteria as important indicator of water quality, ecotoxicology or biotechnological applications, (E) fungi for air quality, agriculture or aquatic food webs, (F) particulate matter for air quality, (G) microplastics as pollutants in air, water and food, (H) organelles as starch granules for archeology and (I) ploidy for biological conservation and restoration ecology [Color figure can be viewed at [wileyonlinelibrary.com](https://onlinelibrary.wiley.com/doi/10.1002/cyto.a.21658)]

comparable to existing time-series datasets. Thirdly, multispectral imaging flow cytometry also allows the simultaneous detection of multiple fluorescence emission patterns per particle, which can be important for identification purposes. For example, pigment-related autofluorescence of cells and particles provides a multispectral fingerprint that can allow better taxonomic discrimination between species or particle types compared to existing bright-field-based imaging flow cytometry systems or only flow cytometry [7]. Finally, in addition to the multi-spectral properties, the microscopic images themselves can be classified with deep learning neural networks for automated recognition and with greater reliability than manual methods [7–9]. Several of the applications presented here are also partially possible with imaging flow cytometry, which provides only brightfield images, for example with tomographic IFC [10], Imaging FlowCytobot [11], CytoSense [12] or FlowCAM [13]. However, fluorescence staining or derivation of spectral taxonomic classes are not possible. Furthermore, automated image recognition with only one channel is much more difficult, whereas multispectral information allows more comprehensive particle characterization. So far a commonly used MIFC instrument is the ImageStream X MkII [14], but similar instruments like the FlowSight or the STEAM flow cytometer exist [14, 15].

While the MIFC method has proven to be promising, so far it has not been widely applied. Therefore, we aim to provide an overview in this paper of potential applications of MIFC to environmental monitoring and different biological organism groups of interests as well as best practice recommendations (Table 1). In this article we show exemplary data derived from an ImageStream X Mk II (Amnis part of Luminex—A DiaSorin Company, Texas, Austin) MIFC instrument equipped with three lasers (488, 561, and 785 nm), 20x, 40x and 60x magnification, two CCD cameras and 12 detector channels. The instrument is what we have available, but the presented applications

are definitely not restricted to the specific instrument type, any MIFC instrument with the specific requirements could be used.

1.1 | Fields of application for environmental multispectral imaging flow cytometry monitoring

1.1.1 | Air quality and bioaerosol assessment

Allergology

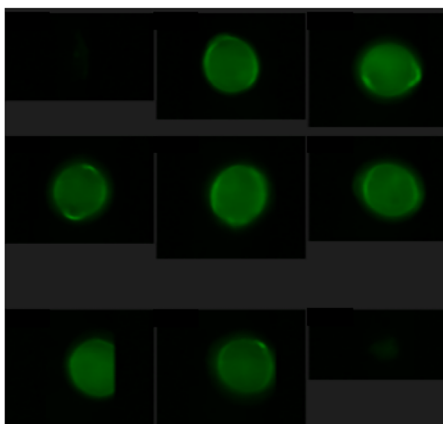
Pollen analysis as part of air quality assessment is traditionally performed with manual microscopy and is of relevance for pollen forecasts [20]. Allergically most important plants are birch (*Betula* sp.), alder (*Alnus* sp.), hazel (*Corylus* sp.), grasses (Poaceae) and—recently of growing interest—the invasive ragweed (*Ambrosia* sp.) [21]. Each plant pollen has a species-specific morphology and besides those most important plant pollen, up to 100 different other pollen types may be present in the air. A differentiation of this large number is only feasible to a limited extent with manual microscopic counting.

Some approaches exist that apply automated microscopic imaging of pollen, however they only include brightfield images [22–24]. In previous work it could be shown that pollen analysis could be also performed with MIFC [9] and in addition to pollen identification alone, MIFC (including brightfield images and fluorescence images) allows the measurement of allergen content per pollen based on fluorescence-labeled antibodies (Figure 2).

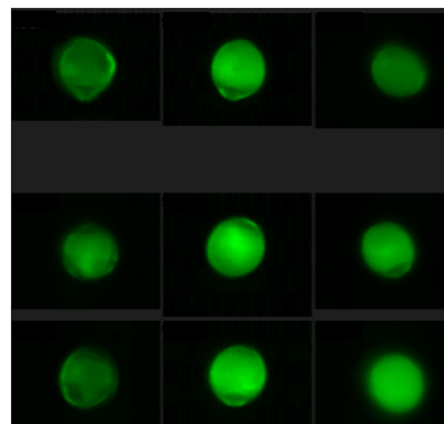
In several studies, it could be shown that for clinical relevance of allergy symptoms, the pollen concentration is only a rough proxy, as the allergen content per pollen can greatly differ [25–27]. Different amounts of major allergens per pollen may be detected as a function of plant growth, land use, climate/weather events, plant's microbiome

FIGURE 2 Allergen staining of birch (*Betula* sp.) pollen. *Betula* sp. pollen (40x magnification) collected in Leipzig, Germany with their autofluorescence (A) and labeled with a polyclonal BETV1A antibody (FITC), IgG, rabbit (Biozol, Eching, Germany) (B). Fluorescence was measured with Ex. 488 nm/Em. 528/65 nm [Color figure can be viewed at [wileyonlinelibrary.com](https://onlinelibrary.wiley.com)]

Unstained birch pollen
(FITC channel)



Bet v1-stained birch pollen
(FITC channel)



or pollution [21]. Therefore, in addition to conventional pollen traps, imaging flow cytometry can help to analyze pollen in more detail, that is, with regard to their allergenicity.

The broad size spectrum of MIFC covering 20 nm [28] up to 270 μm also allows a detailed particle analysis of air samples, including particulate matter fractions, fungal spores and algae. A more detailed prediction of pollen diversity in combination with particulate matter, based on multispectral information, could potentially allow for an improved allergy medication therapy.

Ice nucleating particles

Linked to meteorological research, the source identification of ice-nucleating particles (INPs), is of relevance to better understand climate effects of cloud and ice particle formation. INPs are airborne particles, which influence the phase (liquid or ice), the radiative properties and precipitation behavior of clouds [29]. An important sub-group of INPs are primary particles of biogenic origin such as pollen, spores emitted or fragments from plants, fungi, algae and lichen, as well as bacteria becoming air-borne through the dispersion of, for example, plant fragments and soil particles [29, 30]. MIFC allows to measure these types of particles from for example air or rain water samples. Autofluorescent pigments of phototrophic organisms, particles or fragments allow easy differentiation from all other particle types in the samples. Biogenic particles are known to trigger the heterogeneous freezing of cloud droplets at much higher temperatures than, for example, INP consisting of mineral dust [29]. INP type and concentration may therefore have an influence on local weather and climate, and knowledge on them is crucial to improve and constrain climate models [31].

Current INP determination is either done via online (applying, e.g., a continuous flow diffusion chamber [32] or offline methods (filter sampling and subsequent analysis in a freezing array [33]). However, knowledge on the INP type (mineral vs. biogenic) can only be gained via the offline method and there indirectly via heating or chemical treatment with H_2O_2 of the sample [34]. The biogenic material is degraded by the treatment and the effect on the sample's freezing spectra is recorded. These degrading methods allow only to

conclude that the INP population included heat-labile biogenic material (i.e., proteins) or H_2O_2 -labile material (i.e., organic material in general), but not which biogenic species acted as INP. Combining MIFC with the offline INP methods would allow for a specific identification of ice active particles from selected biogenic sources.

1.1.2 | Water quality assessment

Phytoplankton is traditionally investigated by manual microscopical investigations for several areas of water quality assessment (freshwater, marine and ballast water) as it is a crucial part of the biological quality component in all directives and conventions like the *EU Water Framework Directive* (WFD—https://ec.europa.eu/environment/water/water-framework/info/intro_en.htm), the *EU Bathing Water Directive* (2006/7/EC) (https://ec.europa.eu/environment/water/water-bathing/index_en.html), the *EU Marine Strategy Framework Directive* (MSFD—https://ec.europa.eu/environment/marine/eu-coast-and-marine-policy/marine-strategy-framework-directive/index_en.htm) or the *Ballast Water Management convention* (BWM—<https://www.imo.org/en/OurWork/Environment/Pages/BWMConventionandGuidelines.aspx>) to guarantee a good quality of European water bodies. Therefore, intercalibration activities were started in the past years to harmonize water quality assessment across Europe.

The *EU Water Framework Directive* aims at monitoring freshwater ecosystems (rivers and lakes), while the *EU Marine Strategy Framework Directive* was put in place to protect the marine ecosystem and biodiversity upon which our health, economic and social activities depend on. The bathing water quality is monitored according to the *EU Bathing Water Directive* and includes freshwater and marine systems. The *Ballast Water Management convention* aims to prevent the spread of harmful aquatic organisms from one region to another and halt damage to the marine environment from ballast water discharge, by minimizing the uptake and subsequent discharge of sediments and organisms. From 2024, all ships are required to have an approved Ballast Water Management Treatment System, which requires control of

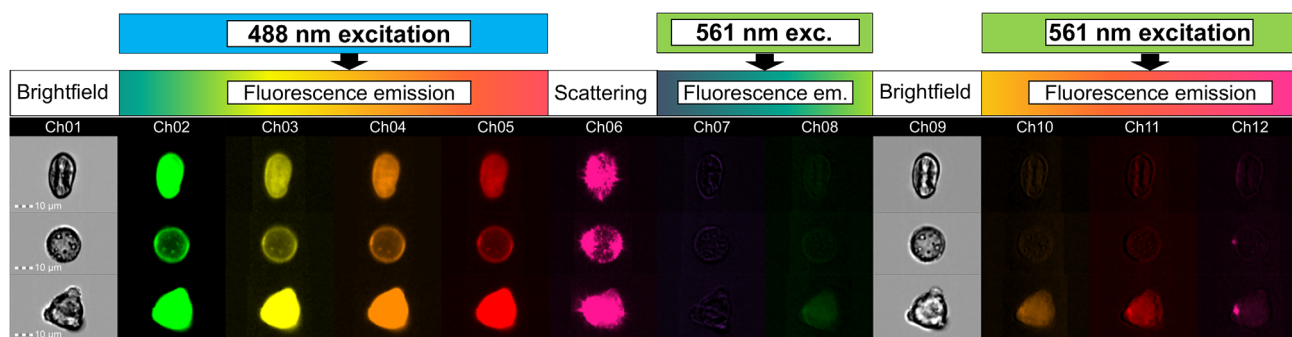


FIGURE 3 Pollen from honey samples collected at Fürstenrieder Schloss (Munich, Germany). Multispectral microscopic images (40x magnification) of one particle in each row for different channels. Brightfield channels (Ch01/Ch09), fluorescence image channels of different spectral ranges: Ch02—Ex. 488 nm/Em. 528/65 nm, Ch03—Ex. 488 nm/Em. 577/35 nm, Ch04—Ex. 488 nm/Em. 610/30 nm, Ch05—Ex. 488 nm/Em. 702/85 nm, Ch07—Ex. 561 nm/Em. 457/45 nm, Ch08—Ex. 561 nm/Em. 537/65 nm, Ch10—Ex. 561 nm/Em. 610/30 nm, Ch11—Ex. 561 nm/Em. 702/85 nm, Ch12—Ex. 561 nm/Em. 762/35 nm and scatter channel (Ch06 Ex. 785 nm). Sample preparation was according to DIN 10760 [Color figure can be viewed at [wileyonlinelibrary.com](https://onlinelibrary.wiley.com/doi/10.1002/cyto.a.24658)]

the ballast water of every ship in a harbor. In addition, toxic phytoplankton monitoring is relevant for water treatment facilities, aquaculture facilities or biotechnological process control (section 1.1.7).

Similarly to air quality assessment, the sample throughput for water quality assessment is limited by manual microscopy and expert knowledge is required to identify the different organisms of interest accordingly. Due to this bottleneck, many alternative methods have been developed in the past few years [4–6, 8, 11, 35, 36]. Many instruments only use brightfield images to classify phytoplankton species of interest, but it could be recently demonstrated that MIFC could provide more robust species classifications by combining spectral properties and classified images [7, 37] (Figure 6). Furthermore, fluorescence in situ hybridization techniques (FISH) could be applied to specifically identify certain problematic taxa [38].

Assessment of toxicological effects on microalgae

Microalgae are used in standardized test systems to assess adverse effects of chemicals on growth and reproduction of cell populations. To increase the throughput of cell counting, classical methods like coulter counter or microscopy were recently replaced by flow cytometry [39]. However, flow cytometry offers many more options beyond the assessment of cell numbers. Fluorochrome labeling allows the analysis of physiological processes of cells. Fluorescent markers for membrane permeability and potential, mitochondrial respiration and esterase activity were used to identify different modes of action of toxins in microalgae [40] and to evidence the induction of reactive oxygen species by natural polyphenols [41]. By using synchronized algal cultures resulting in populations with all cells in a comparable growth stage, deviations from normal growth could be assessed by flow cytometry [42] and MIFC would offer an even more robust identification of comprised cell clusters.

1.1.3 | Food quality assessment

The EU Honey Directive (2001/110/EC) aims at preserving the purity of honey as an unprocessed natural agricultural product. Honey needs

to contain a certain amount of a specific pollen to be marketed as variety-specific honey. In addition, a certain percentage of foreign pollen allows the determination of the quality and botanical and geographical origin of the honey, which is an important step of food quality control performed by national authorities [43–45]. More sensitive and high-throughput honey analysis may even enhance identification and consequently reduce honey adulteration or mislabeling (Figure 3). Currently, as with the other monitoring tasks, this is done via manual microscopy, but pollen classification could be demonstrated with MIFC as well [9]. Additionally, non-biological contamination of honey by fibers and microplastic [46], as well as biological contamination via spores of bee disease causing agents [47] or by spores of microbial plant protection products (some examples listed here: [48] and their potential effects on bees and humans, can be investigated and quantified using MIFC.

1.1.4 | Paleoecology

For paleo-botany, sediment analysis allows reconstructing past vegetation and climate by analysis of pollen or phytoplankton residuals. Starch granules are of relevance in archeological research to explore diet and cultural practices of early humans. In both of these disciplines, manual microscopy is still the gold standard.

Traditional pollen analyses, where about 300–1000 pollen grains in a sample are analyzed using a light microscope is time-consuming (several hours per sample) and requires expert knowledge and is strongly biased by the pollen analyst background and experience. In this regard, the development of MIFC as a new tool for automated fossil pollen identification would be promising, because many more grains could be identified (Figure 4). This is of particular interest as, compared to the pollen source vegetation, the pollen composition in the fossil sample is highly skewed toward wind-pollinated tree taxa. A higher total pollen count would also retrieve the rare taxa often originating from insect-pollinated herbs and would thus allow for a more accurate interpretation of the pollen record with respect to the past

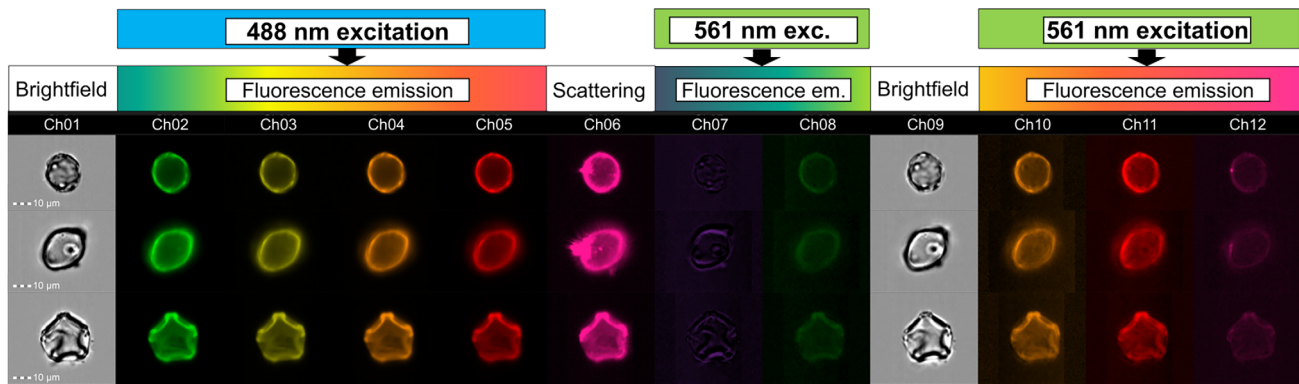


FIGURE 4 ~6000-year-old pollen from a sediment core of Lake Rauchagytygn, North-East Siberia. Multispectral microscopic images (40x magnification) of one particle in each row for different channels. Brightfield channels (Ch01/Ch09), fluorescence image channels of different spectral ranges: Ch02—Ex. 488 nm/Em. 528/65 nm, Ch03—Ex. 488 nm/Em. 577/35 nm, Ch04—Ex. 488 nm/Em. 610/30 nm, Ch05—Ex. 488 nm/Em. 702/85 nm, Ch07—Ex. 561 nm/Em. 457/45 nm, Ch08—Ex. 561 nm/Em. 537/65 nm, Ch10—Ex. 561 nm/Em. 610/30 nm, Ch11—Ex. 561 nm/Em. 702/85 nm, Ch12—Ex. 561 nm/Em. 762/35 nm and scatter channel (Ch06 Ex. 785 nm) [Color figure can be viewed at [wileyonlinelibrary.com](https://onlinelibrary.wiley.com)]

plant composition. Pollen records are available from thousands of sites (<https://www.neotomadb.org/>) and most analysts keep their pollen samples (typically stored in glycerin) after analyses. Such the development of cytometry as a new method could potentially make use of tens of thousands of available samples.

Modern diatom assemblages show strong species-environment relationships and are valuable biological indicators. Because diatom shells (frustules) preserve in sediments, past assemblages of diatoms are largely applied for paleoenvironmental reconstructions of, for example, past hydrochemistry [49–51], past temperature and climate [50, 52, 53] and ecological and trophic status [54–56] of freshwater and marine habitats. Diatom frustules show distinctive morphological features that allow classifications to low taxonomic levels with light microscopy. However, subtle but ecologically important morphological differences are often only identifiable by scanning electron microscopy [57]. Generally, microscopic identification of diatom assemblages requires expert knowledge and is very time-consuming (about 300–500 diatom frustules will be taxonomically determined and counted per sample). Automated identification of modern diatom samples (water samples and culture collections) using imaging flow cytometry already provided promising results [7, 8], but needs to be tested on more complex samples, like marine sediments. Modern reference specimens, which will be used to train the identification algorithms, are needed beforehand to establish robust identification in automated MIFC. Diatom samples are typically prepared in water solutions and are largely cleaned from organic material and sediment particles, however broken frustules, which are typical for sediment samples due to taphonomic processes, will be hard to identify. Specialized algorithms are needed to classify diagnostic pieces of frustules, which may result in classifications to higher taxonomic levels (e.g., genus) only. Chrysophyte cysts are used similarly to diatom frustules in paleolimnological studies to elucidate past environmental conditions in lakes. They pose the additional challenges that diagnostic structures can be very delicate and many fossil forms have no modern analogs. However, the analysis of large cyst populations using flow cytometry has recently

demonstrated that even their size distribution can be a valuable proxy for historic ecological conditions [58].

1.1.5 | Pollination ecology

Most wild plant and crop species rely on the interactions with animal pollinators for reproduction [59]. We must understand how plant-pollinator interactions and the services they provide respond to global change factors such as climate and land use in order to manage ecosystems and secure pollination services. The strength of interactions between plants and pollinators is the product of both the quantity (number of visits by pollinators to plants) and quality (number of pollen grains delivered per visit) of interactions. Pollinator visitation (quantity of visits) is typically measured observationally, as the rate at which pollinator species come into contact with the reproductive parts of the flower and could potentially perform pollination. However, visitation rate is not always a good measure of the efficiency of insects as pollinators. Measuring pollen transport (quality of visits) by counting the number and identity of pollen grains on the bodies of pollinators or on the stigma of flowers, thereby provides a far better estimate of the pollination efficiency of various insect species in removing and delivering pollen to flowering plants. Assessing pollen transport can thus provide direct insights into the impact of anthropogenic change on pollination as an ecosystem service.

Despite the importance of measuring pollen transport, few studies in pollination ecology have observed and quantified pollen transport networks [60–64]. This is because the identification and counting of pollen grains is typically conducted by ecologists using microscopy, which is time-consuming and requires expert knowledge in palynology. Identifying pollen using meta-barcoding has been shown to have high pollen species identification accuracy, but poor estimation of the absolute pollen numbers of different species [1]. Previous attempts using flow cytometry that measured only scatter and fluorescence properties could not distinguish many pollen species, and were

particularly challenged when dealing with closely related species [65, 66]. Thus, the field of pollination ecology has been limited by methods for rapid and accurate pollen identification and quantification.

A recent study using MIFC with deep learning revealed fast (~2000 images per second) and accurate (~96% accuracy) identification of 35 insect-dispersed pollen species [9], including close relatives. This opens up opportunities for assessing plant-pollinator interactions across broad spatial and temporal environmental gradients, which are necessary to understand responses to global change. Further, there are numerous new opportunities for understanding phylogenetic patterns in pollen traits, derived from the MIFC images and addressing new questions about angiosperm macroevolution.

Studying plant-pollinator interactions by analysis of pollen from individual insects will help to identify for example, “pollinator-friendly” seed mixes for meadows or meadow strips that are increasingly used in urban areas or agriculture fields to increase food and nesting resources of insects and therewith biodiversity [67].

1.1.6 | Agriculture

In agricultural research, selection of relevant genotypes is an important task for food safety. In this context, plant ploidy (2.3.1) and pollen vitality (2.3.3) are of relevance to be determined. Similarly relevant is the detection of phytopathogens (2.4).

Processes in soils are difficult to assess, but the ratio of photoautotrophic (algae, lichens, plant fragments or spores) to heterotrophic biomass (fungal spores or bacteria), could be a relevant measure to better understand global change effects on soil health, functioning and biodiversity. Autotrophs as soil algae have been technically difficult to quantify and thus are less well studied than soil heterotrophic organisms like bacteria or fungi. Based on a study by Hunt et al. [68], the role of soil algae should not be neglected, as abundances can be quite high, equivalent to soil fungi and only one or two orders of magnitude lower than actinomycetes and bacteria. So far, microscopic soil particles are not measured routinely with MIFC, but Lentendu et al. [69] provided a useful protocol for isolation, quantification and vitality assessment of autotrophic and heterotrophic soil organisms with flow cytometry, which could be further explored with MIFC.

1.1.7 | Process control in microbial biotechnology

The application of MIFC in microbial biotechnology focuses on three aspects: (1) semi-online biological process control; (2) detection of infections and risk management; (3) real-time information about the physiological status of the productive cells. Huang [70] showed the application of MIFC in the optimization process of biomass formation of *Pichia burtonii* mainly based on the analysis of the surface scattering of the cells. In microalgal biotechnology, the process control is a big challenge because the cells are normally exposed to natural environmental conditions with respect to light and temperature. Both conditions strongly influence the growth performance and ask for

regulation of different parameters for example, mixing energy, CO₂ or nutrient delivery [71]. The main potential of MIFC in algal biotechnology is the detection of contaminations (Figure 6), especially on quantitative terms. The high efficiency in cell differentiation by image and spectral analysis can be further improved by the combination with in situ hybridization, which allows to identify even unwanted mutations in the community [72]. The future development in MIFC will allow to collect specific physiological information in large scale photobioreactors. For instance, toxic interaction between bacteria in algae, for example *Pseudomonas protegens* and the green alga *Chlamydomonas reinhardtii* disturb the Ca-homeostasis in the green cell [73] which can be monitored by MIFC as shown in T-cells [74]. This approach does not only allow to monitor infections but also to analyze the reasons for decreased algal growth performance. If MIFC is combined with Vibrational spectroscopy like Raman [75] or single cells can be analyzed with single-cell-fourier-transform-infrared (FTIR) spectroscopy methods to the status of the cell cycle [76], the ratio of dead and living cells [77] and the cellular quantity of lipids [78]. The lipids can be quantified also using the dye Nile Red using MIFC as analyzing instrument. Since the FTIR spectrum can be used as a fingerprint for the actual growth potential of an algal cell [79] FTIR combined with MIFC has the potential of quasi simultaneous online analysis of growth rates and product concentrations.

1.1.8 | Microplastic research

Microplastic particles in water, drinks and food, soil, air samples or plants are a serious concern for ecosystem and human health [80–82]. Particles in the range of 1–100 µm are of special interest, as their size-related effects on food webs need to be better understood. Small environmental microplastics cannot be identified by microscopy alone, current gold standards are micro-Raman spectroscopy or micro-FTIR spectroscopy [83, 84]. This requires specialized equipment, experienced personnel, long sample preparation time and spectra analysis. Generally, the majority of natural particles needs to be removed from the samples before microplastic detection. In addition, the practical lower size limit of single particle analysis is in the micrometer range. Therefore, fluorescently labeled spherical microplastics are typically used in uptake studies or toxicological experiments. As one such application employing flow cytometry, microplastic phagocytosis by immune cells has been recently studied [85]. Small microplastics made from various polymers may be stained with Nile Red to be accessible for flow cytometric detection down to a size limit of 200 nm [86]. Flow cytometry combined with visual Stochastic Neighbor Embedding (visNE) algorithms allowed the detection of few microplastic particles against the cellular background of a highly diverse stream biofilm community [87]. If experiments include microplastic particle fractions with known morphology and size spectrum, MIFC may allow evaluation of very high numbers of (even unstained) particles in a shorter time compared to spectroscopic methods (Figure 5). This approach may allow detection of changes in size spectrum or typical morphologies in a particle population.

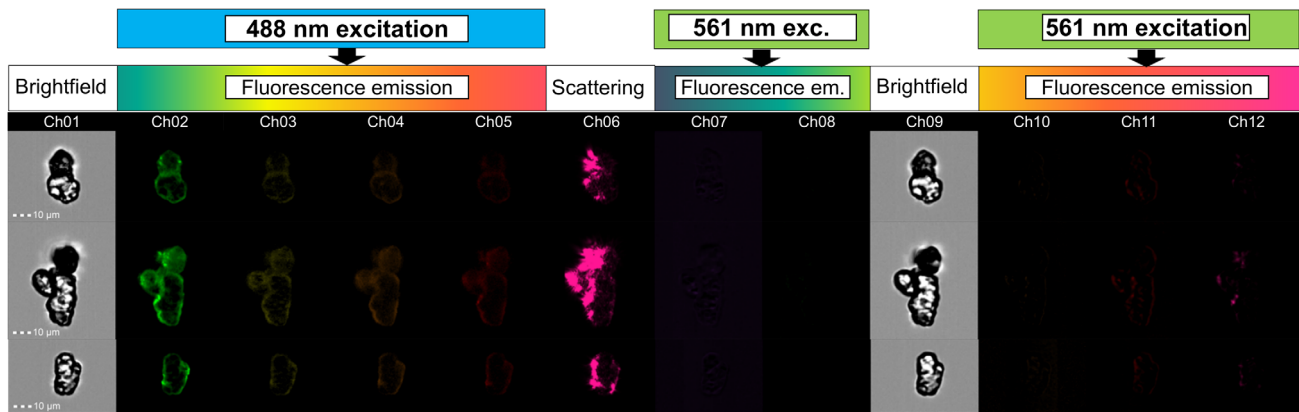


FIGURE 5 Microplastic particles. Multispectral microscopic images (40x magnification) of one particle in each row for different channels. Brightfield channels (Ch01/Ch09), fluorescence image channels of different spectral ranges: Ch02—Ex. 488 nm/Em. 528/65 nm, Ch03—Ex. 488 nm/Em. 577/35 nm, Ch04—Ex. 488 nm/Em. 610/30 nm, Ch05—Ex. 488 nm/Em. 702/85 nm, Ch07—Ex. 561 nm/Em. 457/45 nm, Ch08—Ex. 561 nm/Em. 537/65 nm, Ch10—Ex. 561 nm/Em. 610/30 nm, Ch11—Ex. 561 nm/Em. 702/85 nm, Ch12—Ex. 561 nm/Em. 762/35 nm and scatter images (Ch06 Ex. 785 nm) of polyamide particles used in a microplastic research project (MikroPlaTaS <https://bmbf-plastik.de/de/verbundprojekt/mikroplatas>). [Color figure can be viewed at [wileyonlinelibrary.com](https://onlinelibrary.wiley.com)]

2 | ORGANISMS OF INTEREST FOR ENVIRONMENTAL MIFC

2.1 | Algae and cyanobacteria

Phytoplankton organisms can be differentiated according to their different pigmentation and morphology [7, 37]. Diversity of phytoplankton organisms in terms of community structure and biomass is crucial for our well-being in form of drinking water quality or recreational activities and is therefore monitored in the WFD, MFSD and BWM. As primary producer, phytoplankton organisms plays also a major role for any aquatic ecosystem. For that reason, phytoplankton organisms are also an ideal tool for experimental studies, for example of multidimensional niches [88] or species interactions [89] (Figure 6). Aeroterrestrial algae and cyanobacteria can be important for air quality issues as a fraction of bioaerosols or meta-community studies and soil algae can contribute to soil fertilization and stabilization [68]. In addition, biotechnological systems with microalgae can be easily and regularly monitored with MIFC for purity and potential contaminations.

2.2 | Bryophytes

Bryophytes (mosses, liverworts, hornworts) are widespread plants in many ecosystems and regarded as sensitive to environmental stresses [90] and thus they are frequently used in environmental monitoring [91]. There are at least two main benefits of using MIFC in bryophyte-based research and monitoring. First, MIFC is powerful to count numbers of spores and vegetative diaspores, as well as to assess variation in pigmentation and size (Figure 7). Second, MIFC enables rapid quantitative analysis of the species composition of epiphytic microbiota on bryophyte surfaces (green algae, cyanobacteria) that can be sensitive to environmental conditions and anthropogenic nutrient deposition or

climatic conditions. Flow cytometry has been used to measure DNA content [92, 93] and ploidy level of bryophytes [94, 95].

2.3 | Vascular plants

Ferns are the second largest group of vascular plants. They reproduce with spores and are a useful model for plant research as they can act as a miniaturized and thus economic higher plant model, for example, for environmental toxicity monitoring [96]. Besides the quantification of spore numbers, several biomarkers of toxicological bioassays can be derived by MIFC, for example mitochondrial activity, chlorophyll fluorescence, DNA content and oxidative damage [97]. An advantage of higher plants in contrast to certain phytoplankton species is, that they have a low fluorescence emission in the green spectral region (“green gap”) allowing for the application of fluorescence dyes in this region [98]. Furthermore, ploidy and genome size (2.3.1), plant organelles (2.3.2), starch granules (2.3.3) or pollen (2.3.4) can be nicely visualized and investigated in detail with MIFC.

2.3.1 | Ploidy and genome size

In the evolutionary history of higher plants, polyploidy, that is, whole genome duplication, is an important macroevolutionary mechanism as all modern plant genomes are the result of repeated polyploidization events [99]. Polyploidy often results in immediate reproduction isolation and speciation and thus is a major driver of biodiversity. In many taxa, closely related di-, tetra-, hexa- or octoploid races coexist, differently taxonomically recognized at the levels of species, subspecies or as intraspecific variation.

Different ploidy levels differ in genome size, physiological capacity and cell dimensions. Therefore, chromosome races may differ in life history traits, fitness at particular environmental conditions, and in

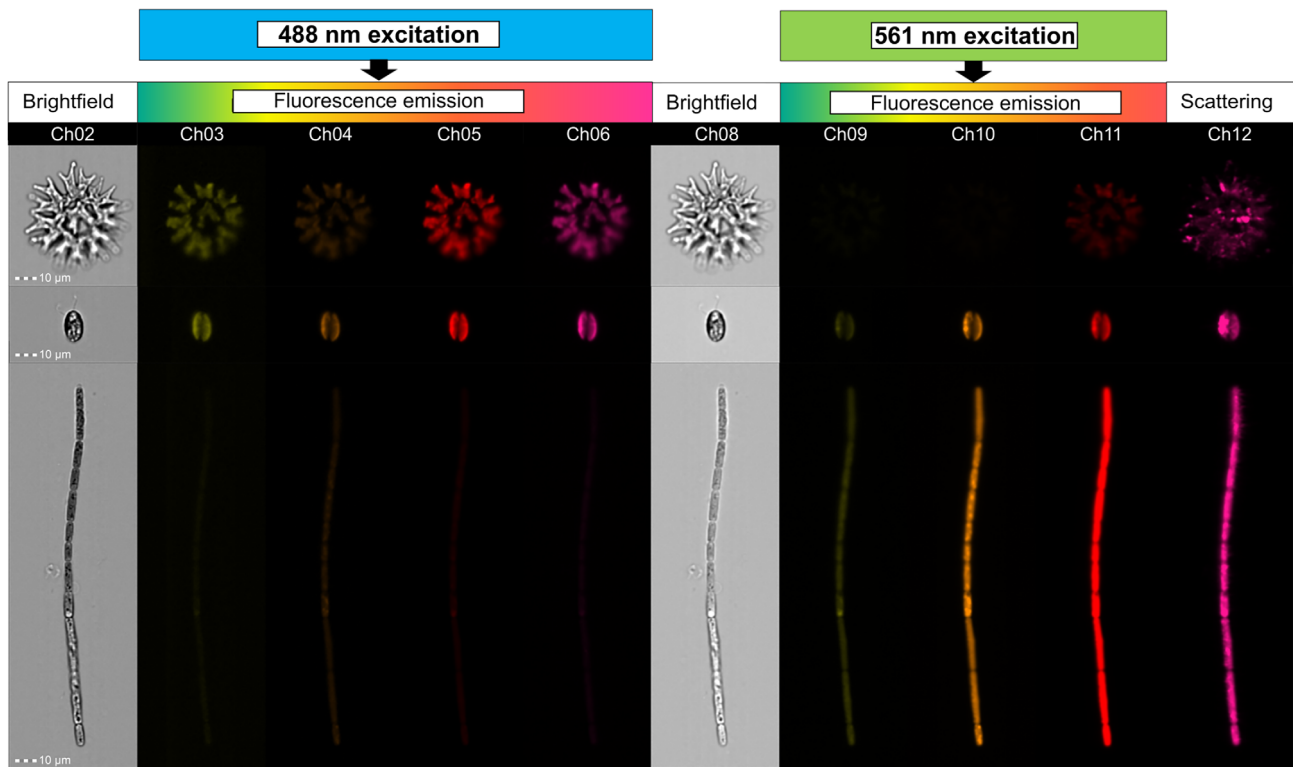


FIGURE 6 Algae and cyanobacteria. Some exemplary algae as (A) *Pediastrum biradiatum*, (B) *Cryptomonas ovata* and a cyanobacterium (C) *Anabaena flos-aquae* being relevant for the monitoring of the EU water framework directive. Multispectral microscopic images (40x magnification) of one particle in each row for different channels. Brightfield channels (Ch02/Ch08), fluorescence image channels of different spectral ranges: Ch03—Ex. 488 nm/Em. 577/35 nm, Ch04—Ex. 488 nm/Em. 610/30 nm, Ch05—Ex. 488 nm/Em. 702/85 nm, Ch09—Ex. 561 nm/Em. 582/35 nm, Ch10—Ex. 561 nm/Em. 610/30 nm, Ch11—Ex. 561 nm/Em. 702/85 nm and scatter channel (Ch12 Ex. 785 nm). [Color figure can be viewed at wileyonlinelibrary.com]

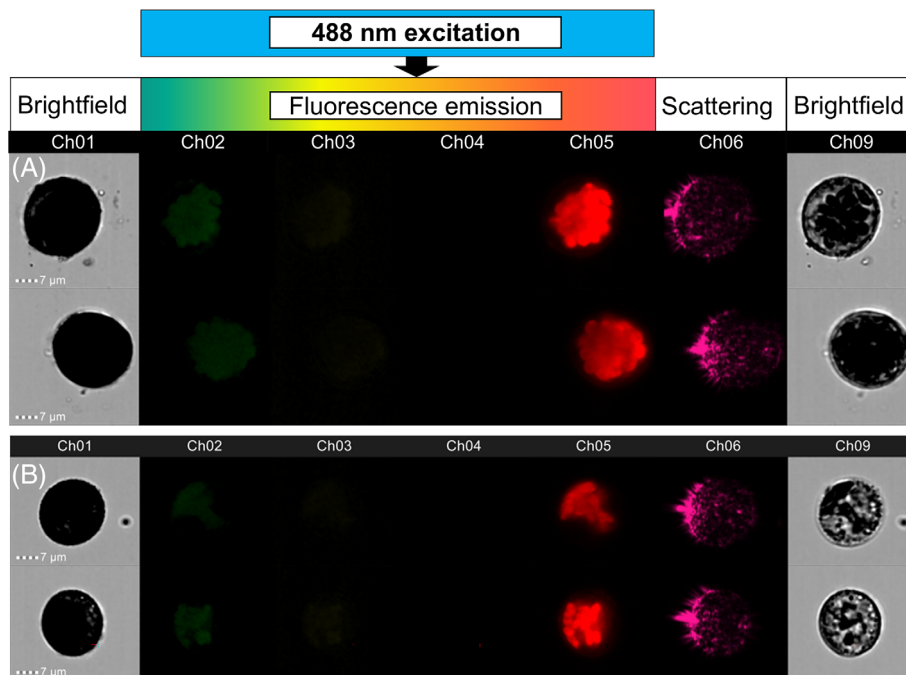


FIGURE 7 Bryophyte spores. Multispectral microscopic images (40x magnification) of one particle in each row for different channels. Brightfield image channels (Ch01/Ch09), fluorescence image channels of different spectral ranges: Ch02—Ex. 488 nm/Em. 528/65 nm, Ch03—Ex. 488 nm/Em. 577/35 nm, Ch04—Ex. 488 nm/Em. 610/30 nm, Ch05—Ex. 488 nm/Em. 702/85 nm and scatter channel (Ch06 Ex. 785 nm) of the species (A) *Dicranum* sp. and (B) *Rhytidiadelphus* sp. collected at Lotharpfad, Black Forest National Park, Germany. [Color figure can be viewed at wileyonlinelibrary.com]

biotic interactions, potentially resulting in ploidy-specific niches or distribution patterns. However, the distribution patterns of intraspecific chromosome races are often unknown [100].

In biological conservation and restoration ecology, intraspecific chromosome races need to be accounted for in order not to obliterate natural distribution patterns and their likely adaptedness. In European

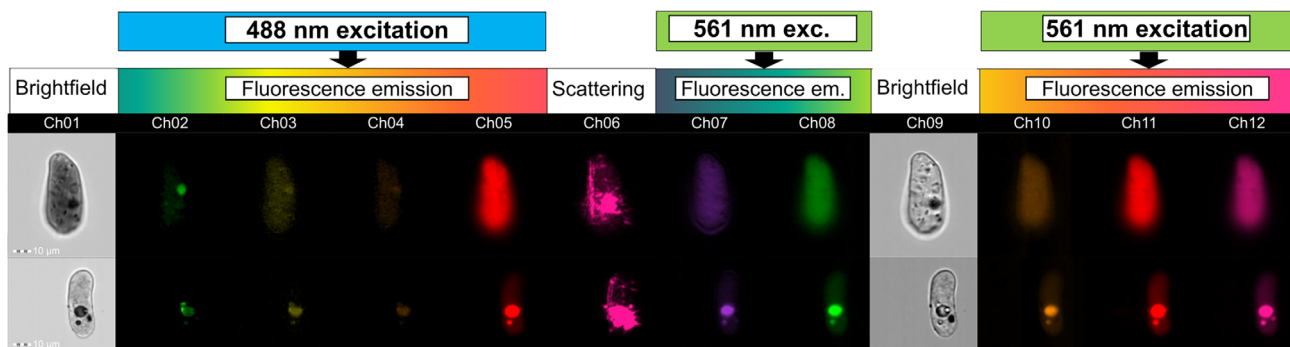


FIGURE 8 Plant cells. Multispectral microscopic images (40x magnification) of one particle in each row for different channels. Brightfield channels (Ch01/Ch09), fluorescence image channels of different spectral ranges: Ch02—Ex. 488 nm/Em. 528/65 nm, Ch03—Ex. 488 nm/Em. 577/35 nm, Ch04—Ex. 488 nm/Em. 610/30 nm, Ch05—Ex. 488 nm/Em. 702/85 nm, Ch07—Ex. 561 nm/Em. 457/45 nm, Ch08—Ex. 561 nm/Em. 537/65 nm, Ch10—Ex. 561 nm/Em. 610/30 nm, Ch11—Ex. 561 nm/Em. 702/85 nm, Ch12—Ex. 561 nm/Em. 762/35 nm and scatter channel (Ch06 Ex. 785 nm) of *Centaurea* sp. cells, treated with RNase and stained with Sytox (Ch02). [Color figure can be viewed at wileyonlinelibrary.com]

grasslands, for example, diploid and tetraploid races of *Knautia arvensis* (Dipsacaceae), which do not differ morphologically, are strongly genetically differentiated and show regional adaptation [101]. Consequently, seed transfer zones for the production of regional seed material for grassland restoration should account for these distribution patterns making ploidy screening or genetic analyses necessary across putative seed transfer zones. As a standardized method, plant ploidy is determined by extracting nuclei from plant cell tissue and DNA-staining with respective dyes [102] (Figure 8). Alternatively, pollen size should also be an indicator of ploidy. MIFC allows for both, nuclei visualization and quantification, as well as for pollen size determination.

2.3.2 | Organelles

Organelle extraction of tissue is more often applied routinely for human or animal tissue, while plant material has some unique features (rigid cell walls, interfering secondary metabolites, autofluorescence) which makes its analyses by flow cytometry more challenging [19]. Despite these specific features, many protocols have been developed to extract plant or algae organelles like chloroplast, thylakoids, nuclei, autolysosomes or mitochondria from tissue samples [19, 103, 104]. They can further be used for deeper understanding of evolutionary, biochemical and physiological processes [105], for example chloroplasts have different morphology and fluorescence pattern in C3- and C4-plants [106] or proteoms [105].

2.3.3 | Starch granules

In archeology, starch grain analysis is employed to track how economic plants—especially cultigens—were used [107, 108] and spread (e.g., [109–112] in antiquity. This is because many economically important plant taxa produce large amounts of starch [113], which, through sheer amount, may persist. Additionally, some depositional contexts not conducive to good organic preservation, such as

extremely acidic soils, preferentially preserve starch [114]. In the Canadian Subarctic, for example, bone and non-carbonized organic remains tend to be very sparse in archeological sites due to shallow and acid soils, yet starch granules from food plants have been routinely recovered from soil and food residues in this region [111, 112, 115, 116].

Despite the promise of archeological starch in the reconstruction of past foodways, starch morphology is highly complicated, and reliable identification criteria are only available for a narrow range of taxa [117–121]. Although attempts have been made to create dichotomous keys for starch (e.g., [113]), identification is problematic due to intraspecies variability [122]; shared morphotypes and size overlap between disparate species [118]; and inconsistencies in descriptive language used to record discrete characteristics [117]. Since morphotypes can number in the dozens, or more per species, traditional dichotomous keys are rendered either overly specific, when leading to only one morphotype per species [113] or frustratingly cumbersome, when leading to all possible types [115].

Due to the inherent morphological complexity of starch, and the large number of specimens that may potentially be recovered from archeological contexts, the creation of an identification key for starch granules is an ideal application for MIFC combined with machine learning. This is because, to properly capture the intraspecies variation and identification criteria of starch, up to 350 individual granules must be measured per species [123]. Depending on the number of measured variables, this can be prohibitively labor intensive when analyzing several (e.g., $n = 15$) species using low throughput microscopy [124]. MIFC in combination with machine learning is capable of collecting these measurements quickly, while also objectively recording discrete characteristics of starch granules (Figure 9).

2.3.4 | Pollen

Plant pollen morphology is species specific and can help to analyze honey, pollinator-plant interactions, as well as allergic wind-

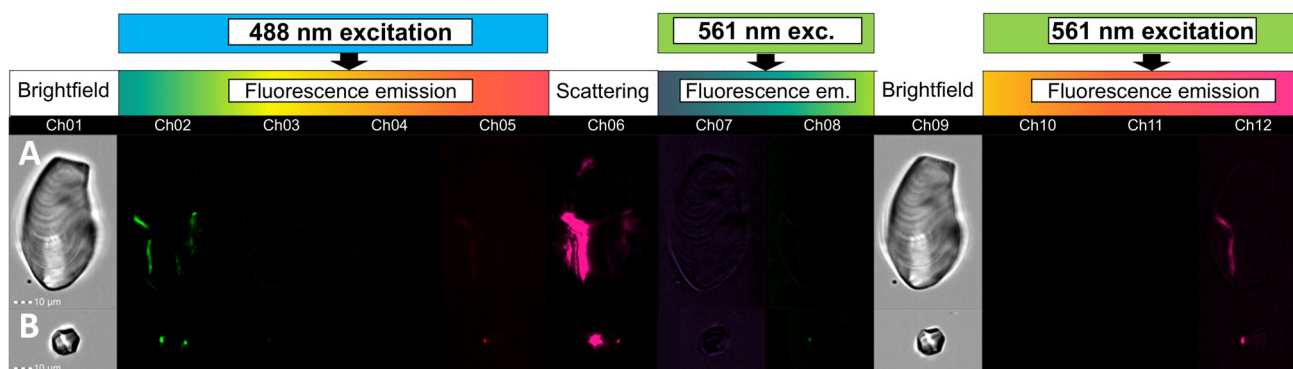


FIGURE 9 Plant starch granules. Multispectral microscopic images (40x magnification) of one particle in each row for different channels. Brightfield channels (Ch01/Ch09), fluorescence image channels of different spectral ranges: Ch02—Ex. 488 nm/Em. 528/65 nm, Ch03—Ex. 488 nm/Em. 577/35 nm, Ch04—Ex. 488 nm/Em. 610/30 nm, Ch05—Ex. 488 nm/Em. 702/85 nm, Ch07—Ex. 561 nm/Em. 457/45 nm, Ch08—Ex. 561 nm/Em. 537/65 nm, Ch10—Ex. 561 nm/Em. 610/30 nm, Ch11—Ex. 561 nm/Em. 702/85 nm, Ch12—Ex. 561 nm/Em. 762/35 nm and scatter images (Ch06 Ex. 785 nm) of starch granules from *Musa* sp. (A) and *Zea mays* (B). [Color figure can be viewed at [wileyonlinelibrary.com](https://onlinelibrary.wiley.com/doi/10.1002/cyto.a.24658)]

distributed pollen (see sections 1.1.3, 1.1.4, 1.1.6, and 1.1.1, respectively). An overview of recent developments of using flow cytometry in pollen analyses is provided by Kron et al., [125]. Automation of pollen analyses has been a research focus since the 1990s [126, 127] mainly for its multiple facets in different research areas [128] for example as application in fossil pollen analyses (1.1.4) but also for plant-pollinator interactions (1.1.3/1.1.6) and aerial pollen monitoring (1.1.1). With respect to fossil pollen analyses both the imaging techniques as well as the image data analysis techniques have been targeted. While data analysis techniques, in particular neural network, supported the breakthrough in automated fossil pollen identification from images [129], the process of image collection from the fossil samples is still not yet automated. MIFC has not yet become a standard technique in fossil pollen analysis, while standard analytical flow cytometry and (on-chip) sorting have been already applied to collect fossil pollen grains from sediments for radiocarbon dating [66, 130].

Samples from pollen traps can further be used to monitor flowering phenology of plants (especially wind pollinated species) as the timepoint of pollen release is an important part of flowering phenology. Other plant traits such as plant height, specific leaf area or leaf nitrogen content and growth forms [131, 132] are related to phenological timing as well. Studying of phenology is of high relevance as shifts in flowering phenology are a sensitive indicator of climate change [133]. Flower phenology is further associated with other phenological stages, such as leaf senescence, in many species [134, 135], and the timing of pollen release can therefore be used to extract additional information on the life cycle of plants and as indicator of climate change.

2.4 | Phytopathogenic fungi

Fungi can be analyzed by MIFC to assess their important roles in aquatic and terrestrial diversity and food webs, as phytopathogens or in the primary bioaerosol fraction. Infection of phytoplankton species

by parasitic saprophytic fungi (e.g., Chytridiomycota) is an important part of aquatic trophic interactions [136, 137] and the detection of *Asterionella* infections by Rhizophydiales fungi using a Wheat germ agglutinin marker for fungal cell walls has revealed comparable results for microscopy and MIFC [137]. This allows the pathway of the destructive aquatic food web, to be studied in greater detail and with higher throughput. Phytopathogenic fungi can cause huge crop losses [138] and especially in sustainable organic farming biocontrol and monitoring of plant pathogens will get more important as a lower level of agrochemicals is applied [139]. Potential phytopathogenic and allergically relevant airborne fungi were shown to be measured with conventional flow cytometry based on propidium iodide [140] or calcofluor staining [141]. MIFC will also allow more specific automatic sizing and accurate assignment to different fungi morpho-types. In addition, *Saccharomyces cerevisiae* is studied as a model organism for cell cycle analysis and this can be well performed with MIFC [142].

3 | DATA AND IMAGE ANALYSIS TO ASSESS PARTICLE IDENTIFICATION

From the perspective of data processing and analysis MIFC also poses some very specific opportunities and challenges. Measurement data is typically captured as still images with 6–12 channels of 16-bit color depth having a rather low resolution of 120-pixel width. These images arrive with a rate of up to 5000 particles/s meaning that a typical measurement captures between 72.000 and 720.000 images per hour. Thereby, the objects of the same particle type will likely be captured from different perspectives. Since particles will be resolved in a fluid suspension (e.g., Dulbecco's Phosphate Buffered Saline buffer), a variation in the production of these chemicals may impact image appearance and has to be considered when analyzing images. The machine itself is recalibrated every measurement day to counterbalance such effects, but we still found them relevant when designing an analysis pipeline for training of deep neural networks.

Once measurements have been performed, several potential analysis approaches exist: (1) detection, that is, finding an object of interest in the image and regressing a bounding box around it potentially with subsequent classification of the object; (2) classification, that is, identifying the depicted particle(s) and (3) feature analysis, for example deriving continuous values representing characteristics (traits) of the particle such as size, shape, texture signal strength and location features. We already captured large datasets of phytoplankton and pollen and successfully trained models for their identification [8, 9] and performed feature analysis [9]. The typical choice for this kind of problem are convolutional neural networks (CNN) with a large variety of individual algorithms/architectures depending on the data size, available training data and computational resources. What makes the design and training of these networks specific for MIFC data is (1) the analysis of multi-spectral, that is, multi-channel, data that differs from the three-color channel images typically analyzed with these architectures, and (2) capturing characteristics that are very stable within a measurement sequence but may substantially differ among different measurement campaigns and require careful training set orchestration and training regularization such as data augmentation.

To support and accelerate future research it would be desirable to have a reusable training pipeline with alternative model architectures and an analysis guideline aggregating best practices in the field. At the same time, it would be incredibly helpful to have a benchmark consisting of multiple rich datasets referring to common applications of MIFC. Such a benchmark could stimulate more research into specific machine learning methods and to compare developed solutions.

4 | CHALLENGES AND LIMITATIONS

So far, the upper size range of the MIFC instrument presented is limited to 100 μm diameter of a spherical particle. It could be shown that the maximum diameter of elongated or filamentous cells possible to measure could be much higher than 100 μm , for example up to 270 μm for filamentous cells. But besides some large pollen (e.g., of Malvaceae, Onagraceae or Pinaceae) with a size up to 190 μm and very large phytoplankton cells that cannot be measured due to the size limitation, a very large fraction of the groups of organisms described in this manuscript can be surveyed with MIFC. With a lower size range of 20 nm even really small bacteria with a minimum size of 0.1 μm [143] can be investigated.

In contrast to other monitoring applications of air or water quality, MIFC as presented here does not allow for online-monitoring, as the instrument is a lab instrument not suitable for field operation. However, several core facilities are equipped with MIFC instruments like the ImageStream X Mk II or the FlowSight (Amnis part of Lumindex—A DiaSorin Company, Texas, Austin) and offer service time to run samples. In contrast to many online monitoring tasks, MIFC measurements of benchtop instruments allow for a deeper level of analysis with respect to species recognition and physiology because of better image quality and higher magnification. In addition, the

sample preparation procedure allows for addition of various fluorescent dyes to identify or quantify certain cell/particle properties.

Despite the impressive range of applications, it is recommended that MIFC is compared with the gold standard microscopy for a representative sample subset during the establishment of any new procedure, to gain confidence in the applications and to guarantee that particle properties are suitable for MIFC measurements.

With respect to deep learning approaches based on MIFC images, a problem to overcome in this regard is the typically effort-intensive labeling of training sets, that is, assigning an identification, bounding box or a characteristic value per image, necessary to generate feedback in the training process and to facilitate the learning of a model. Such labels are often manually created making them very expensive, but alternative strategies are in development. Despite the challenges which still need to be addressed with MIFC, the method is the best available and it still poses plenty of opportunities to allow for new analyses and to improve existing analyses, for example, the coverage of a large spectral range could be more intensively used and the high capture speed may even allow for feedback from the analysis process to the actual measurement.

5 | CONCLUSIONS

As demonstrated, MIFC has high potential to be useful for a wide range of environmental monitoring tasks that are currently performed with manual microscopy (e.g., pollen and phytoplankton monitoring) or other analytical approaches (e.g., spectroscopic methods for microplastic detection). MIFC can be meaningful when combined with other species identification methods as metabarcoding and next generation sequencing [2] or is ideally coupled with a sorting option [144]. As the comparability to standard manual microscopic approaches is higher than with chemical or molecular tools, this technique can be more powerful in advancing different environmental monitoring tasks.

6 | BEST PRACTICE RECOMMENDATIONS

General best practice recommendations for environmental multispectral imaging flow cytometric measurements (Table 1):

- For the quantification of any cells or particles, the measured sample volume is determined, but in addition to that it is recommended to use count check beads (e.g., CountBright™ Absolute Counting Beads, ThermoFisher Scientific) as an internal standard.
- The incubation time in fluid suspension of any non-aquatic organism or particle may affect the physiology and phenotype of the particles and should be as short as possible.
- Since MIFC produces a lot of data, it is of particular importance to have appropriate data management strategies in place and to deal with it according to FAIR principles (Findability, Accessibility, Interoperability, Reuse). In addition, standardized archiving of cytometry as well as image data is to be performed.

TABLE 1 Specific best practice recommendations for environmental related multispectral imaging flow cytometric measurements

Objects of interests	Specific recommendations
Pollen	<ul style="list-style-type: none"> • Due to their hydrophobic surface, a suitable pollen isolation buffer [9, 16] should be used to get pollen in a fluid suspension. • Pollen properties are influenced by conditions of storage; therefore, we recommend to either measuring them as soon as possible after collection or to freeze them at -20°C and only defrost them immediately before performing sample preparations for MIFC. At least a minimum of pollen of up to 5000 pollen is required for analysis.
Phytoplankton	<ul style="list-style-type: none"> • It is important to be aware that morphology and pigment composition and thus cell morphology and fluorescence signals are affected by nutrient conditions and light intensities species are exposed to [8]. Therefore, a comparison of different measurements requires information about the light and nutrient conditions the organism has been exposed to. • Similarly, as for pollen, it is recommended to measure the samples as fresh as possible to avoid artifacts due to fixation. • In the case that due to practical reasons fixation is required, we recommend fixation procedures with a glutaraldehyde fixation, freezing in liquid nitrogen and storage at -80°C for delayed analyses [17, 18].
Organelles	<ul style="list-style-type: none"> • The morphology of organelles is dependent to which medium they are exposed, as they are sensitive to any osmotic changes. It will be important to cool the samples, keep incubation times low, and control for that factor by using the same medium for all samples if a comparative assessment is performed. • Samples with nuclei, chloroplasts or mitochondria should be measured as fresh as possible after extraction [19] (1–2 h), while starch granules can be preserved as a powder once extracted and can be stored for longer time in a dry stage.
Deep learning	<ul style="list-style-type: none"> • Building common training datasets and establishing benchmarks for particle-specific identification and recognition tasks. • Development and systematic evaluation of a deep learning pipeline for MIFC.

Abbreviation: MIFC, multispectral imaging flow cytometry.

- To guarantee FAIR principles of data management, we recommend to provide the standardized “Minimum Information about a Flow Cytometry Experiment” (MIFlowCyt) according to the International Society for Analytical Cytology (ISAC) for all experiments and measurements [145–147]. Deposition of image data is currently not included in this MIFlowCyt standard and only includes the required information for a conventional flow cytometry. Some authors raised this issue [146–148], but to the best of our knowledge, none

of these formats are in widespread use yet. We recommend to use internal/institutional databases to sustainably store relevant file formats and/or images and ideally use a DOI system to refer to the respective data.

AUTHOR CONTRIBUTIONS

Susanne Dunker: Funding acquisition (lead); project administration (lead); supervision (lead); visualization (equal); writing – original draft (lead); writing – review and editing (lead). **Matthew Boyd:** Writing – original draft (supporting); writing – review and editing (supporting). **Walter Durka:** Writing – original draft (supporting); writing – review and editing (supporting). **Silvio Erler:** Funding acquisition (lead); writing – original draft (supporting); writing – review and editing (supporting). **Stan Harpole:** Funding acquisition (equal); writing – original draft (supporting); writing – review and editing (supporting). **Silvia Henning:** Writing – original draft (supporting); writing – review and editing (supporting). **Ulrike Herzsich:** Writing – original draft (supporting); writing – review and editing (supporting). **Thomas Hornick:** Project administration (supporting); visualization (equal); writing – original draft (supporting); writing – review and editing (supporting). **Tiffany Marie Knight:** Writing – original draft (supporting); writing – review and editing (supporting). **Stefan Lips:** Writing – original draft (supporting); writing – review and editing (supporting). **Patrick Mäder:** Writing – original draft (supporting); writing – review and editing (supporting). **Elena Motivans Švara:** Writing – original draft (supporting); writing – review and editing (supporting). **Steven Mozarowski:** Writing – original draft (supporting); writing – review and editing (supporting). **Demetra Rakosy:** Writing – original draft (supporting); writing – review and editing (supporting). **Christine Römermann:** Writing – original draft (supporting); writing – review and editing (supporting). **Mechthild Schmitt-Jansen:** Writing – original draft (supporting); writing – review and editing (supporting). **Kathleen Stoof-Leichsenring:** Writing – original draft (supporting); writing – review and editing (supporting). **Frank Stratmann:** Writing – original draft (supporting); writing – review and editing (supporting). **Regina Treudler:** Writing – original draft (supporting); writing – review and editing (supporting). **Risto Virtanen:** Writing – original draft (supporting); writing – review and editing (supporting). **Katrin Wendt-Potthoff:** Writing – original draft (supporting); writing – review and editing (supporting). **Christian Wilhelm:** Writing – original draft (supporting); writing – review and editing (supporting).

ACKNOWLEDGMENTS

The authors thank the German Research Foundation for support via the iDiv Flexpool Funding projects Grant Number: 34600865-16 (“Kick-off-Meeting PolDiv”), Grant Number: 34600830-13, (“PolDiv”-Project) and Grant Number: RA-373/20 (iCyt - Support Unit). Susanne Dunker, Patrick Mäder and Silvio Erler were further supported by the Federal Ministry of Food and Agriculture (BMEL) via the project “NutriBee” (Grant Number: 2819NA066, 2819NA102, 2819NA106), based on a decision of the parliament of the Federal Republic of Germany via the Federal Office for Agriculture and Food (BLE) under

the Federal Programme for Ecological Farming and Other Forms of Sustainable Agriculture (BÖLN). Katrin Wendt-Potthoff was supported by the BMBF project MikroPlaTaS (grant number 02WPL1448A). The authors thank Wolfgang Osswald for providing honey samples for a proof-of-concept study. Open Access funding enabled and organized by Projekt DEAL.

CONFLICT OF INTEREST

Susanne Dunker has the patent submission PCT/EP2017/075553 and a cooperation contract with Luminex Corporation, Austin, Texas which could create a potential conflict of interest. No financial benefit accrued from patent submission until the date of manuscript submission.

DATA AVAILABILITY STATEMENT

The raw data (.rif-files) of the figures presented in this study are available via <https://doi.org/10.48758/ufz.12577>.

ORCID

Susanne Dunker  <https://orcid.org/0000-0001-7276-776X>
 Walter Durka  <https://orcid.org/0000-0002-6611-2246>
 Silvio Erler  <https://orcid.org/0000-0002-9425-8103>
 W. Stanley Harpole  <https://orcid.org/0000-0002-3404-9174>
 Silvia Henning  <https://orcid.org/0000-0001-9267-7825>
 Ulrike Herzschuh  <https://orcid.org/0000-0003-0999-1261>
 Thomas Hornick  <https://orcid.org/0000-0003-0280-9260>
 Tiffany Knight  <https://orcid.org/0000-0003-0318-1567>
 Stefan Lips  <https://orcid.org/0000-0002-2291-6584>
 Elena Motivans Švara  <https://orcid.org/0000-0002-2407-9564>
 Demetra Rakosy  <https://orcid.org/0000-0001-8010-4990>
 Christine Römermann  <https://orcid.org/0000-0003-3471-0951>
 Mechthild Schmitt-Jansen  <https://orcid.org/0000-0002-4541-6515>
 Kathleen Stoof-Leichsenring  <https://orcid.org/0000-0002-6609-3217>
 Frank Stratmann  <https://orcid.org/0000-0003-1977-1158>
 Regina Treudler  <https://orcid.org/0000-0002-9642-4742>
 Risto Virtanen  <https://orcid.org/0000-0002-8295-8217>
 Katrin Wendt-Potthoff  <https://orcid.org/0000-0002-7407-3312>

REFERENCES

- Bell KL, Burgess KS, Botsch JC, Dobbs EK, Read TD, Brosi BJ. Quantitative and qualitative assessment of pollen DNA metabarcoding using constructed species mixtures. *Mol Ecol*. 2019;28(2):431–55. <https://doi.org/10.1111/mec.14840>
- Groendahl S, Kahlert M, Fink P. The best of both worlds: A combined approach for analyzing microalgal diversity via metabarcoding and morphology-based methods. *PLoS One*. 2017;12(2):e0172808. <https://doi.org/10.1371/journal.pone.0172808>
- Barteneva NS, Fasler-Kan E, Vorobjev IA. Imaging flow cytometry: coping with heterogeneity in biological systems. *J Histochem Cytochem*. 2012;60(10):723–33. <https://doi.org/10.1369/0022155412453052>
- Dashkova V, Malashenkov D, Poulton N, Vorobjev I, Barteneva NS. Imaging flow cytometry for phytoplankton analysis. *Methods*. 2017; 112:188–200. <https://doi.org/10.1016/j.ymeth.2016.05.007>
- Poulton, Nicole J. (2016): FlowCam: quantification and classification of phytoplankton by imaging flow cytometry. In Natasha S. Barteneva, Ivan A. Vorobjev, editors. *Imaging flow cytometry. Methods and protocols*. 1st ed. New York, NY: Humana Press (SpringerLink Bücher); 2016. pp. 237–247. https://doi.org/10.1007/978-1-4939-3302-0_17.
- Poulton NJ. Imaging flow cytometry for phytoplankton analysis: instrumentation and applications. *J Biomol Techn*. 2019;30:S52.
- Dunker S. Hidden secrets behind dots: improved phytoplankton taxonomic resolution using high-throughput imaging flow cytometry. *Cytometry A*. 2019;95(8):854–68. <https://doi.org/10.1002/cyto.a.23870>
- Dunker S, Boho D, Wäldchen J, Mäder P. Combining high-throughput imaging flow cytometry and deep learning for efficient species and life-cycle stage identification of phytoplankton. *BMC Ecol*. 2018;18(1):1–15. <https://doi.org/10.1186/s12898-018-0209-5>
- Dunker S, Motivans E, Rakosy D, Boho D, Mäder P, Hornick T, et al. Pollen analysis using multispectral imaging flow cytometry and deep learning. *New Phytol*. 2021;229(1):593–606. <https://doi.org/10.1111/nph.16882>
- Kleiber A, Kraus D, Henkel T, Fritzsche W. Review: tomographic imaging flow cytometry. *Lab Chip*. 2021;21(19):3655–66. <https://doi.org/10.1039/D1LC00533B>
- Sosik HM, Olson RJ. Automated taxonomic classification of phytoplankton sampled with imaging-in-flow cytometry. *Limnol Oceanogr Methods*. 2007;5(6):204–16. <https://doi.org/10.4319/lom.2007.5.204>
- Fragoso GM, Poulton AJ, Pratt NJ, Johnsen G, Purdie DA. Trait-based analysis of subpolar North Atlantic phytoplankton and plastidic ciliate communities using automated flow cytometer. *Limnol Oceanogr*. 2019;64(4):1763–78. <https://doi.org/10.1002/lno.11189>
- Sieracki CK, Sieracki ME, Yentsch CS. An imaging-in-flow system for automated analysis of marine microplankton. *Mar Ecol Prog Ser*. 1998;168:285–96. Available from: <http://www.jstor.org/stable/24828385>
- Rožanc J, Finšgar M, Maver U. Progressive use of multispectral imaging flow cytometry in various research areas. *Analyst*. 2021; 146(16):4985–5007. <https://doi.org/10.1039/D1AN00788B>
- Goda K, Ayazi A, Gossett DR, Sadasivam J, Lonappan CK, Sollier E, et al. High-throughput single-microparticle imaging flow analyzer. *Proc Natl Acad Sci U S A*. 2012;109(29):11630–5. <https://doi.org/10.1073/pnas.1204718109>
- Aloisi, Iris; Cai, Giampiero; Tumiatti, Vincenzo; Minarini, Anna; Del Duca, Stefano (2015): Natural polyamines and synthetic analogs modify the growth and the morphology of *Pyru communis* pollen tubes affecting ROS levels and causing cell death. *Plant Sci* 239, pp. 92–105. DOI: <https://doi.org/10.1016/j.plantsci.2015.07.008>.
- Marie D, Rigaut-Jalabert F, Vaultot D. An improved protocol for flow cytometry analysis of phytoplankton cultures and natural samples. *Cytometry A*. 2014;85(11):962–8. <https://doi.org/10.1002/cyto.a.22517>
- Brussaard CPD, Marie D, Thyraug R, Bratbak G. Flow cytometric analysis of phytoplankton viability following viral infection. *Aquat Microb Ecol*. 2001;26(2):157–66. <https://doi.org/10.3354/ame026157>
- Loureiro J, Doležel J, Greilhuber J, Santos C, Suda J. Plant flow cytometry—far beyond the stone age 73 (A). 2008:579–580. <https://doi.org/10.1002/cyto.a.20578>.
- Bastl K, Berger M, Bergmann K-C, Kmenta M, Berger U. The medical and scientific responsibility of pollen information services. *Wien Klin Wochenschr*. 2017;129(1–2):70–4. <https://doi.org/10.1007/s00508-016-1097-3>
- Marselle MR, Stadler J, Korn H, Irvine KN, Bonn A. In: Marselle MR, Stadler J, Korn H, Irvine KN, editors. *Biodiversity and health in the face of climate change*. Aletta Bonn. Cham: Springer International

- Publishing; 2019 Available from: <https://library.open.org/handle/20.500.12657/22910>
22. Kleiber A, Ramoji A, Mayer G, Neugebauer U, Popp J, Henkel T. 3-Step flow focusing enables multidirectional imaging of bioparticles for imaging flow cytometry. *Lab Chip*. 2020;20(9):1676–86. <https://doi.org/10.1039/D0LC00244E>
 23. Olsson O, Karlsson M, Persson AS, Smith HG, Varadarajan V, Yourstone J, et al. Efficient, automated and robust pollen analysis using deep learning. *Methods Ecol Evol*. 2021;12(5):850–62. <https://doi.org/10.1111/2041-210X.13575>
 24. Oteros J, Pusch G, Weichenmeier I, Heimann U, Möller R, Röseler S, et al. Automatic and online pollen monitoring. *IAA*. 2015;167(3):158–66. <https://doi.org/10.1159/000436968>
 25. Buters J, Prank M, Sofiev M, Pusch G, Albertini R, Annesi-Maesano I, et al. Variation of the group 5 grass pollen allergen content of airborne pollen in relation to geographic location and time in season. *J Allergy Clin Immunol*. 2015;136(1):87–95.e6. <https://doi.org/10.1016/j.jaci.2015.01.049>
 26. Buters JTM, Kasche A, Weichenmeier I, Schober W, Klaus S, Traidl-Hoffmann C, et al. Year-to-year variation in release of bet v 1 allergen from birch pollen: evidence for geographical differences between west and South Germany. *IAA*. 2008;145(2):122–30. <https://doi.org/10.1159/000108137>
 27. Buters JTM, Thibaudon M, Smith M, Kennedy R, Rantio-Lehtimäki A, Albertini R, et al. Release of Bet v 1 from birch pollen from 5 European countries. Results from the HIALINE study. *Atmos Environ*. 2012;55:496–505. <https://doi.org/10.1016/j.atmosenv.2012.01.054>
 28. Headland SE, Jones HR, D'Sa ASV, Perretti M, Norling LV. Cutting-edge analysis of extracellular microparticles using ImageStream(X) imaging flow cytometry. *Sci Rep*. 2014;4(1):5237. <https://doi.org/10.1038/srep05237>
 29. Kanji ZA, Ladino LA, Wex H, Boose Y, Burkert-Kohn M, Cziczko DJ, et al. Overview of ice nucleating particles. *Meteorol Monogr*. 2017;58(1):1.1-1.33. <https://doi.org/10.1175/AMSMONOGRAPHS-D-16-0006.1>
 30. Huang S, Hu W, Chen J, Wu Z, Zhang D, Fu P. Overview of biological ice nucleating particles in the atmosphere. *Environ Int*. 2021;146:106197. <https://doi.org/10.1016/j.envint.2020.106197>
 31. Vergara-Temprado J, Miltenberger AK, Furtado K, Grosvenor DP, Shipway BJ, Hill AA, et al. Strong control of Southern Ocean cloud reflectivity by ice-nucleating particles. *Proc Natl Acad Sci U S A*. 2018;115(11):2687–92. <https://doi.org/10.1073/pnas.1721627115>
 32. Rogers DC, DeMott PJ, Kreidenweis SM, Chen Y. A continuous-flow diffusion chamber for airborne measurements of ice nuclei. *J Atmos Ocean Technol*. 2001;18(5):725–41. [https://doi.org/10.1175/1520-0426\(2001\)018<0725:ACFDCE>2.0.CO;2](https://doi.org/10.1175/1520-0426(2001)018<0725:ACFDCE>2.0.CO;2)
 33. Conen F, Henne S, Morris CE, Alewell C. Atmospheric ice nucleators active ≥ -12 °C can be quantified on PM₁₀ filters. *Atmos Meas Tech*. 2012;5(2):321–7. <https://doi.org/10.5194/amt-5-321-2012>
 34. Tobo Y, DeMott PJ, Hill TCJ, Prenni AJ, Swoboda-Colberg NG, Franc GD, et al. Organic matter matters for ice nuclei of agricultural soil origin. *Atmos Chem Phys*. 2014;14(16):8521–31. <https://doi.org/10.5194/acp-14-8521-2014>
 35. Işıl Ç, de Haan K, Göröcs Z, Koydemir HC, Peterman S, Baum D, et al. Phenotypic analysis of microalgae populations using label-free imaging flow cytometry and deep learning. *ACS Photonics*. 2021;8(4):1232–42. <https://doi.org/10.1021/acsp Photonics.1c00220>
 36. Petruk V, Kvaternyuk S, Yasynska V, Kozachuk A, Kotyra A, Romaniuk RS, Askarova N. The method of multispectral image processing of phytoplankton processing for environmental control of water pollution. In: *Optical Fibers and Their Applications 2015: International Society for Optics and Photonics* (9816), 98161N. 2015. <https://doi.org/10.1117/12.2229202.short>
 37. Dunker S. Imaging flow cytometry for phylogenetic and morphologically based functional group clustering of a natural phytoplankton community over 1 year in an Urban pond. *Cytometry A*. 2020;97(7):727–36. <https://doi.org/10.1002/cyto.a.24044>
 38. Toepel J, Wilhelm C, Meister A, Becker A, Del Martinez-Ballesta MC. *Cytometry of freshwater phytoplankton. Methods in cell biology: cytometry*. Volume 75. 4th ed. San Diego, CA: Academic Press; 2004. pp. 375–407. Available from: <https://www.sciencedirect.com/science/article/pii/S0091679X04750153>
 39. Stauber JL, Franklin NM, Adams MS. Applications of flow cytometry to ecotoxicity testing using microalgae. *Trends Biotechnol*. 2002;20(4):141–3. [https://doi.org/10.1016/S0167-7799\(01\)01924-2](https://doi.org/10.1016/S0167-7799(01)01924-2)
 40. Adler NE, Schmitt-Jansen M, Altenburger R. Flow cytometry as a tool to study phytotoxic modes of action. *Environ Toxicol Chem*. 2007;26(2):297–306. <https://doi.org/10.1897/06-1636R.1>
 41. Eigemann F, Hilt S, Schmitt-Jansen M. Flow cytometry as a diagnostic tool for the effects of polyphenolic allelochemicals on phytoplankton. *Aquat Bot*. 2013;104:5–14. <https://doi.org/10.1016/j.aquabot.2012.10.005>
 42. Gawel A, Seiwert B, Sühnhholz S, Schmitt-Jansen M, Mackenzie K. In-situ treatment of herbicide-contaminated groundwater-feasibility study for the cases atrazine and bromacil using two novel nanoremediation-type materials. *J Hazard Mater*. 2020;393:122470. <https://doi.org/10.1016/j.jhazmat.2020.122470>
 43. Bicudo de Almeida-Muradian L, Monika Barth O, Dietemann V, Eyer M, Da Freitas AS d, Martel A-C, et al. Standard methods for Apis mellifera honey research. *J Apic Res*. 2020;59(3):1–62. <https://doi.org/10.1080/00218839.2020.1738135>
 44. Corvucci F, Nobili L, Melucci D, Grillenzoni F-V. The discrimination of honey origin using melissopalynology and Raman spectroscopy techniques coupled with multivariate analysis. *Food Chem*. 2015;169:297–304. <https://doi.org/10.1016/j.foodchem.2014.07.122>
 45. von der Ohe W, Oddo P, Piana ML, Morlot M, Martin P. Harmonized methods of melissopalynology. *Apidologie*. 2004;35(suppl 1):S18–25. <https://doi.org/10.1051/apido:2004050>
 46. Al Naggari Y, Brinkmann M, Sayes CM, AL-Kahtani SN, Dar SA, El-Seedi HR, et al. Are honey bees at risk from microplastics? *Toxics*. 2021;9(5):109. <https://doi.org/10.3390/toxics9050109>
 47. Mutinelli F. The spread of pathogens through trade in honey bees and their products (including queen bees and semen): overview and recent developments. *Revue scientifique et technique (International Office of Epizootics)*. 2011;30(1):257–71. <https://doi.org/10.20506/rst.30.1.2033>
 48. Matyjaszczyk E. Products containing microorganisms as a tool in integrated pest management and the rules of their market placement in the European Union. *Pest Manag Sci*. 2015;71(9):1201–6. <https://doi.org/10.1002/ps.3986>
 49. Biskaborn BK, Herzschuh U, Bolshiyarov D, Savelieva L, Zibulski R, Diekmann B. Late Holocene thermokarst variability inferred from diatoms in a lake sediment record from the Lena Delta, Siberian Arctic. *J Paleolimnol*. 2013;49(2):155–70. <https://doi.org/10.1007/s10933-012-9650-1>
 50. Pestryakova LA, Herzschuh U, Gorodnichev R, Wetterich S. The sensitivity of diatom taxa from Yakutian lakes (North-Eastern Siberia) to electrical conductivity and other environmental variables. *Polar Res*. 2018;37(1):1485625. <https://doi.org/10.1080/17518369.2018.1485625>
 51. Pestryakova LA, Herzschuh U, Wetterich S, Ulrich M. Present-day variability and Holocene dynamics of permafrost-affected lakes in central Yakutia (Eastern Siberia) inferred from diatom records. *Quat Sci Rev*. 2012;51:56–70. <https://doi.org/10.1016/j.quascirev.2012.06.020>
 52. Biskaborn BK, Herzschuh U, Bolshiyarov D, Savelieva L, Diekmann B. Environmental variability in northeastern Siberia during the last ~ 13,300 yr inferred from lake diatoms and sediment-geochemical parameters. *Palaeogeogr Palaeoclimatol Palaeoecol*. 2012;329-330:22–36. <https://doi.org/10.1016/j.palaeo.2012.02.003>

53. Hoff U, Rasmussen TL, Meyer H, Koç N, Hansen J. Palaeoceanographic reconstruction of surface-ocean changes in the southern Norwegian Sea for the last ~130,000 years based on diatoms and with comparison to foraminiferal records. *Palaeogeogr Palaeoclimatol Palaeoecol.* 2019;524:150–65. <https://doi.org/10.1016/j.palaeo.2019.03.006>
54. Cumming BF, Laird KR, Gregory-Eaves I, Simpson KG, Sokal MA, Nordin RN, et al. Tracking past changes in lake-water phosphorus with a 251-lake calibration dataset in British Columbia: tool development and application in a multiproxy assessment of eutrophication and recovery in Osoyoos Lake, a transboundary lake in Western North America. *Front Ecol Evol.* 2015;3:84. <https://doi.org/10.3389/fevo.2015.00084>
55. Luoto TP, Nevalainen L, Kauppila T, Tammelin M, Sarmaja-Korjonen K. Diatom-inferred total phosphorus from dystrophic Lake Arapisto, Finland, in relation to Holocene paleoclimate. *Quat Res.* 2012;78(2):248–55. <https://doi.org/10.1016/j.yqres.2012.05.009>
56. Sochuliaková L, Sienkiewicz E, Hamerlík L, Svitok M, Fidlerová D, Bitušík P. Reconstructing the trophic history of an alpine Lake (high Tatra Mts.) using subfossil diatoms: disentangling the effects of climate and human influence. *Water Air Soil Pollut.* 2018;229(9):289. <https://doi.org/10.1007/s11270-018-3940-9>
57. Stoof-Leichsenring KR, Bernhardt N, Pestryakova LA, Epp LS, Herzschuh U, Tiedemann R. A combined paleolimnological/genetic analysis of diatoms reveals divergent evolutionary lineages of *Staurosira* and *Staurosirella* (Bacillariophyta) in Siberian lake sediments along a latitudinal transect. *J Paleolimnol.* 2014;52(1–2):77–93. <https://doi.org/10.1007/s10933-014-9779-1>
58. Siver PA. Potential use of chrysophyte cyst morphometrics as a tool for reconstructing ancient lake environments. *Nova Suppl.* 2019;148:101–12. <https://doi.org/10.1127/nova-suppl/2019/115>
59. Ollerton J, Winfree R, Tarrant S. How many flowering plants are pollinated by animals? *Oikos.* 2011;120(3):321–6. <https://doi.org/10.1111/j.1600-0706.2010.18644.x>
60. Alarcán R. Congruence between visitation and pollen-transport networks in a California plant-pollinator community. *Oikos.* 2010;119(1):35–44. <https://doi.org/10.1111/j.1600-0706.2009.17694.x>
61. Bosch J, González AM, Rodrigo A, Navarro D. Plant-pollinator networks: adding the pollinator's perspective. *Ecol Lett.* 2009;12(5):409–19. <https://doi.org/10.1111/j.1461-0248.2009.01296.x>
62. de Manincor N, Hautekèete N, Mazoyer C, Moreau P, Piquot Y, Schatz B, et al. How biased is our perception of plant-pollinator networks? A comparison of visit- and pollen-based representations of the same networks. *Acta Oecol.* 2020;105:103551. <https://doi.org/10.1016/j.actao.2020.103551>
63. Patiny S. *Evolution of plant-pollinator relationships.* Cambridge, UK: Cambridge University Press; 2011.
64. Pomon A, Andalo C, Burrus M, Escaravage N. DNA metabarcoding data unveils invisible pollination networks. *Sci Rep.* 2017;7(1):16828. <https://doi.org/10.1038/s41598-017-16785-5>
65. Kron P, Husband BC. Using flow cytometry to estimate pollen DNA content: improved methodology and applications. *Ann Bot.* 2012;110(5):1067–78. <https://doi.org/10.1093/aob/mcs167>
66. Tennant RK, Jones RT, Brock F, Cook C, Turney CSM, Love J, et al. A new flow cytometry method enabling rapid purification of fossil pollen from terrestrial sediments for AMS radiocarbon dating. *J Quat Sci.* 2013;28(3):229–36. <https://doi.org/10.1002/jqs.2606>
67. Hicks DM, Ouvrard P, Baldock KCR, Baude M, Goddard MA, Kunin WE, et al. Food for pollinators: quantifying the nectar and pollen resources of Urban flower meadows. *PLoS One.* 2016;11(6):e0158117. <https://doi.org/10.1371/journal.pone.0158117>
68. Hunt ME, Floyd GL, Stout BB. Soil algae in field and forest environments. *Ecology.* 1979;60(2):362–75. <https://doi.org/10.2307/1937665>
69. Lentendu G, Hübschmann T, Müller S, Dunker S, Buscot F, Wilhelm C. Recovery of soil unicellular eukaryotes: an efficiency and activity analysis on the single cell level. *J Microbiol Methods.* 2013;95(3):463–9. <https://doi.org/10.1016/j.jmimet.2013.05.006>
70. Huang J. Application of *Agaricus bisporus* industrial wastewater to produce the biomass of *Pichia burtonii*. *Water Sci Technol.* 2019;79(12):2271–8. <https://doi.org/10.2166/wst.2019.228>
71. Sastre R, Posten C. Optimization of photosynthesis by reactor design. In: Hallmann A, Rampelotto PH, editors. *Photosynthesis biotechnological applications with microalgae.* Cham, Switzerland: De Gruyter STEM; 2021. <https://doi.org/10.1515/9783110716979-007>
72. Brawley J, George T, Hall B, Jorgenson R, Frost K, Perry D et al. Fluorescent in situ hybridization in suspension analysis using ImageStream multispectral imaging flow cytometry. 2008. Available from: <http://dp.univ.it/~laudanna/systems%20biology/technologies/imagestream/posters/fish%20analysis%20using%20imagestream.pdf>.
73. Rose MM, Scheer D, Hou Y, Hotter VS, Komor AJ, Aiyar P, et al. The bacterium *Pseudomonas protegens* antagonizes the microalga *Chlamydomonas reinhardtii* using a blend of toxins. *Environ Microbiol.* 2021;23(9):5525–40. <https://doi.org/10.1111/1462-2920.15700>
74. Cerveira J, Begum J, Barros DM, van der Veen AG, Filby A. An imaging flow cytometry-based approach to measuring the spatiotemporal calcium mobilisation in activated T cells. *J Immunol Methods.* 2015;423:120–30. <https://doi.org/10.1016/j.jim.2015.04.030>
75. Watson DA, Brown LO, Gaskill DF, Naivar M, Graves SW, Doorn SK, et al. A flow cytometer for the measurement of Raman spectra. *Cytometry A.* 2008;73(2):119–28. <https://doi.org/10.1002/cyto.a.20520>
76. Bedolla DE, Kenig S, Mitri E, Storici P, Vaccari L. Further insights into the assessment of cell cycle phases by FTIR microspectroscopy. *Vib Spectrosc.* 2014;75:127–35. <https://doi.org/10.1016/j.vibspec.2014.08.007>
77. Reimann R, Zeng B, Jakopc M, Burdukiewicz M, Petrick I, Schierack P, et al. Classification of dead and living microalgae *Chlorella vulgaris* by bioimage informatics and machine learning. *Algal Res.* 2020;48:101908. <https://doi.org/10.1016/j.algal.2020.101908>
78. Signori L, Ami D, Posterri R, Giuzzi A, Mereghetti P, Porro D, et al. Assessing an effective feeding strategy to optimize crude glycerol utilization as sustainable carbon source for lipid accumulation in oleaginous yeasts. *Microb Cell Factories.* 2016;15(1):75. <https://doi.org/10.1186/s12934-016-0467-x>
79. Fanesi A, Wagner H, Wilhelm C. Phytoplankton growth rate modelling: can spectroscopic cell chemotyping be superior to physiological predictors? *Proc Biol Sci.* 2017;284:20161956. <https://doi.org/10.1098/rspb.2016.1956>
80. Li L, Luo Y, Li R, Zhou Q, Peijnenburg WJGM, Yin N, et al. Effective uptake of submicrometre plastics by crop plants via a crack-entry mode. *Nat Sustain.* 2020;3(11):929–37. <https://doi.org/10.1038/s41893-020-0567-9>
81. Long M, Paul-Pont I, Hégaret H, Moriceau B, Lambert C, Huvet A, et al. Interactions between polystyrene microplastics and marine phytoplankton lead to species-specific hetero-aggregation. *Environ Pollut.* 2017;228:454–63. <https://doi.org/10.1016/j.envpol.2017.05.047>
82. Renner KO, Foster HA, Routledge EJ, Scrimshaw MD. A comparison of different approaches for characterizing microplastics in selected personal care products. *Environ Toxicol Chem.* 2021;41:880–7. <https://doi.org/10.1002/etc.5057>
83. Anger PM, Esch E v d, Baumann T, Elsner M, Niessner R, Ivleva NP. Raman microspectroscopy as a tool for microplastic particle analysis. *TRAC Trends Anal Chem.* 2018;109:214–26. <https://doi.org/10.1016/j.trac.2018.10.010>
84. Primpke S, Fischer M, Lorenz C, Gerdt G, Scholz-Böttcher BM. Comparison of pyrolysis gas chromatography/mass spectrometry and hyperspectral FTIR imaging spectroscopy for the analysis of

- microplastics. *Anal Bioanal Chem.* 2020;412(30):8283–98. <https://doi.org/10.1007/s00216-020-02979-w>
85. Park Y, Abihssira-García IS, Thalmann S, Wiegertjes GF, Barreda DR, Olsvik PA, et al. Imaging flow cytometry protocols for examining phagocytosis of microplastics and bioparticles by immune cells of aquatic animals. *Front Immunol.* 2020;11:203. <https://doi.org/10.3389/fimmu.2020.00203>
 86. Kaile N, Lindivat M, Elio J, Thuestad G, Crowley QG, Hoell IA. Preliminary results from detection of microplastics in liquid samples using flow cytometry. *Front Mar Sci.* 2020;7:856. <https://doi.org/10.3389/fmars.2020.552688>
 87. Sgier L, Freimann R, Zupanic A, Kroll A. Flow cytometry combined with viSNE for the analysis of microbial biofilms and detection of microplastics. *Nat Commun.* 2016;7(1):11587. <https://doi.org/10.1038/ncomms11587>
 88. Hofmann P, Chatzinotas A, Harpole W, Dunker S. Temperature and stoichiometric dependence of phytoplankton traits. *Ecology.* 2019;100(12):e02875. <https://doi.org/10.1002/ecy.2875>
 89. Dunker S, Jakob T, Wilhelm C. Contrasting effects of the cyanobacterium *Microcystis aeruginosa* on the growth and physiology of two green algae, *Oocystis marsonii* and *Scenedesmus obliquus*, revealed by flow cytometry. *Freshw Biol.* 2013;58(8):1573–87. <https://doi.org/10.1111/fwb.12143>
 90. Virtanen R, Eskelinen A, Harrison S. Comparing the responses of bryophytes and short-statured vascular plants to climate shifts and eutrophication. *Funct Ecol.* 2017;31(4):946–54. <https://doi.org/10.1111/1365-2435.12788>
 91. Mallen-Cooper M, Cornwell WK. A systematic review of transplant experiments in lichens and bryophytes. *Bryologist.* 2020;123(3):444–54. <https://doi.org/10.1639/0007-2745-123.3.443>
 92. Ostendorf AK, van Gessel N, Malkowsky Y, Sabovljevic MS, Rensing SA, Roth-Nebelsick A, et al. Polyploidization within the Funariaceae—a key principle behind speciation, sporophyte reduction and the high variance of spore diameters? *BDE.* 2021;43(1):164–79. <https://doi.org/10.11646/bde.43.1.13>
 93. Reski R, Faust M, Wang XH, Wehe M, Abel WO. Genome analysis of the moss *Physcomitrella patens* (Hedw.) B.S.G. *Mol Gen Genet.* 1994;244(4):352–9. <https://doi.org/10.1007/BF00286686>
 94. Bainard JD, Newmaster SG, Budke JM. Genome size and endopolyploidy evolution across the moss phylogeny. *Ann Bot.* 2020;125(4):543–55. <https://doi.org/10.1093/aob/mcz194>
 95. Goga N, Ručová D, Kolarčík V, Sabovljević M, Bačkor M, Lang I. Usnic acid, as a biotic factor, changes the ploidy level in mosses. *Ecol Evol.* 2018;8(5):2781–7. <https://doi.org/10.1002/ece3.3908>
 96. Catala M, Esteban M, Rodríguez-Gil J-L, Quintanilla LG. Development of a naturally miniaturised testing method based on the mitochondrial activity of fern spores: a new higher plant bioassay. *Chemosphere.* 2009;77(7):983–8. <https://doi.org/10.1016/j.chemosphere.2009.07.080>
 97. Feito R, Valcárcel Y, Catalá M. Biomarker assessment of toxicity with miniaturised bioassays: diclofenac as a case study. *Ecotoxicology.* 2012;21(1):289–96. <https://doi.org/10.1007/s10646-011-0790-2>
 98. Dashkova V, Segev E, Malashenkov D, Kolter R, Vorobjev I, Barteneva NS. Microalgal cytometric analysis in the presence of endogenous autofluorescent pigments. *Algal Res.* 2016;19:370–80. <https://doi.org/10.1016/j.algal.2016.05.013>
 99. Wendel JF. The wondrous cycles of polyploidy in plants. *Am J Bot.* 2015;102(11):1753–6. <https://doi.org/10.3732/ajb.1500320>
 100. Paule J, Gregor T, Schmidt M, Gerstner E-M, Dersch G, Dressler S, et al. Chromosome numbers of the flora of Germany—a new online database of georeferenced chromosome counts and flow cytometric ploidy estimates. *Plant Syst Evol.* 2017;303(8):1123–9. <https://doi.org/10.1007/s00606-016-1362-y>
 101. Durka W, Michalski SG, Berendzen KW, Bossdorf O, Bucharova A, Hermann J-M, et al. Genetic differentiation within multiple common grassland plants supports seed transfer zones for ecological restoration. *J Appl Ecol.* 2017;54(1):116–26. <https://doi.org/10.1111/1365-2664.12636>
 102. Dolezel J, Greilhuber J, Suda J. Estimation of nuclear DNA content in plants using flow cytometry. *Nat Protoc.* 2007;2(9):2233–44. <https://doi.org/10.1038/nprot.2007.310>
 103. Galbraith DW, Harkins KR, Maddox JM, Ayres NM, Sharma DP, Firoozabady E. Rapid flow cytometric analysis of the cell cycle in intact plant tissues. *Science (New York, NY).* 1983;220(4601):1049–51. <https://doi.org/10.1126/science.220.4601.1049>
 104. Satori CP, Kostal V, Arriaga EA. Review on recent advances in the analysis of isolated organelles. *Anal Chim Acta.* 2012;753:8–18. <https://doi.org/10.1016/j.aca.2012.09.041>
 105. Schober AF, Bártulos R, Bischoff A, Lepetit B, Gruber A, Kroth PG. Organelle studies and proteome analyses of mitochondria and plastids fractions from the diatom *Thalassiosira pseudonana*. *Plant Cell Physiol.* 2019;60(8):1811–28. <https://doi.org/10.1093/pcp/pcz097>
 106. Pfündel E, Meister A. Flow cytometry of protoplasts from C4 plants. *Photosynthesis: mechanisms and effects.* Dordrecht: Springer; 1998. p. 4341–4. https://doi.org/10.1007/978-94-011-3953-3_1004
 107. Hanson KE, Bryant PL, Painter AM, Skibo JM. Acorn processing and pottery use in the upper Great Lakes: an experimental comparison of Stone boiling and ceramic technology. *Ethnoarchaeology.* 2019;11(2):170–85. <https://doi.org/10.1080/19442890.2019.1642574>
 108. Louderback LA, Pavlik BM. Starch granule evidence for the earliest potato use in North America. *Proc Natl Acad Sci U S A.* 2017;114(29):7606–10. <https://doi.org/10.1073/pnas.1705540114>
 109. Albert RK, Kooiman SM, Clark CA, Lovis WA. Earliest MICROBOTANICAL evidence for maize in the northern Lake MICHIGAN basin. *Am Antiq.* 2018;83(2):345–55. <https://doi.org/10.1017/aaq.2018.10>
 110. Berman MJ, Pearsall DM. Crop dispersal and Lucayan tool use: investigating the creation of transported landscapes in the Central Bahamas through starch grain, Phytolith, macrobotanical, and artifact studies. *J Field Archaeol.* 2020;45(5):355–71. <https://doi.org/10.1080/00934690.2020.1740958>
 111. Boyd M, Surette C, Nicholson BA. Archaeobotanical evidence of prehistoric maize (*Zea mays*) consumption at the northern edge of the Great Plains. *J Archaeol Sci.* 2006;33(8):1129–40. <https://doi.org/10.1016/j.jas.2005.12.003>
 112. Boyd M, Varney T, Surette C, Surette J. Reassessing the northern limit of maize consumption in North America: stable isotope, plant microfossil, and trace element content of carbonized food residue. *J Archaeol Sci.* 2008;35(9):2545–56. <https://doi.org/10.1016/j.jas.2008.04.008>
 113. Messner TC. *Acorns and bitter roots. Starch grain research in the prehistoric eastern woodlands.* Tuscaloosa: University of Alabama Press; 2011.
 114. Langejans GHJ. Remains of the day-preservation of organic micro-residues on stone tools. *J Archaeol Sci.* 2010;37(5):971–85. <https://doi.org/10.1016/j.jas.2009.11.030>
 115. Lints A. Early evidence of maize (*Zea mays* ssp. *mays*) and beans (*Phaseolus vulgaris*) on the northern plains: an examination of Avonlea cultural materials (AD 300–1100). Early evidence of maize (*Zea mays* ssp. *mays*) and beans (*Phaseolus vulgaris*) on the northern plains: an examination of Avonlea cultural materials (AD 300–1100). 2013. Available from: <http://lurepository.lakeheadu.ca/handle/2453/403>.
 116. Zarrillo S, Kooyman B. Evidence for berry and maize processing on the Canadian Plains from starch grain analysis. *Am Antiq.* 2006;71(3):473–99. <https://doi.org/10.1017/S0002731600039779>
 117. Brown GH, Louderback LA. Identification of starch granules from oak and grass species in the central coast of California. *J Archaeol Sci Rep.* 2020;33:102549. <https://doi.org/10.1016/j.jasrep.2020.102549>
 118. Mercader J, Abtosway M, Bird R, Bundala M, Clarke S, Favreau J, et al. Morphometrics of starch granules from sub-Saharan plants

- and the taxonomic identification of ancient starch. *Front Earth Sci.* 2018;6:146. <https://doi.org/10.3389/feart.2018.00146>
119. Musaubach MG, Plos A, Del Babet MP. Differentiation of archaeological maize (*Zea mays* L.) from native wild grasses based on starch grain morphology. Cases from the Central Pampas of Argentina. *J Archaeol Sci.* 2013;40(2):1186–93. <https://doi.org/10.1016/j.jas.2012.09.026>
 120. Perry L, Quigg MJ. Starch remains and Stone boiling in the Texas panhandle part II: identifying Wildrye (*Elymus* spp.). *Plains Anthropol.* 2011;56(218):109–19. <https://doi.org/10.1179/pan.2011.011>
 121. Yang X, Perry L. Identification of ancient starch grains from the tribe Triticeae in the North China plain. *J Archaeol Sci.* 2013;40(8):3170–7. <https://doi.org/10.1016/j.jas.2013.04.004>
 122. Field JH, Kealhofer L, Cosgrove R, Coster ACF. Human-environment dynamics during the Holocene in the Australian wet tropics of NE Queensland: A starch and phytolith study. *J Anthropol Archaeol.* 2016;44:216–34. <https://doi.org/10.1016/j.jaa.2016.07.007>
 123. Holst I, Moreno J, Piperno DR. Identification of teosinte, maize, and *Tripsacum* in Mesoamerica by using pollen, starch grains, and phytoliths. *Proc Natl Acad Sci U S A.* 2007;104(45):17608–13. <https://doi.org/10.1073/pnas.0708736104>
 124. Torrence R, Wright R, Conway R. Identification of starch granules using image analysis and multivariate techniques. *J Archaeol Sci.* 2004;31(5):519–32. <https://doi.org/10.1016/j.jas.2003.09.014>
 125. Kron P, Loureiro J, Castro S, Čertner M. Flow cytometric analysis of pollen and spores: an overview of applications and methodology. *Cytometry A.* 2021;99(4):348–58. <https://doi.org/10.1002/cyto.a.24330>
 126. France I, Duller AWG, Duller GAT, Lamb HF. A new approach to automated pollen analysis. *Quat Sci Rev.* 2000;19(6):537–46. [https://doi.org/10.1016/S0277-3791\(99\)00021-9](https://doi.org/10.1016/S0277-3791(99)00021-9)
 127. Langford M, Taylor GE, Flenley JR. Computerized identification of pollen grains by texture analysis. *Rev Palaeobot Palynol.* 1990;64(1–4):197–203. [https://doi.org/10.1016/0034-6667\(90\)90133-4](https://doi.org/10.1016/0034-6667(90)90133-4)
 128. Hornick T, Richter A, Harpole W, Bastl M, Bohlmann S, Bonn A, et al. An integrative environmental pollen diversity assessment and its importance for the sustainable development goals. *Plants People Planet.* 2021;4:110–21. <https://doi.org/10.1002/ppp3.10234>
 129. Romero IC, Kong S, Fowlkes CC, Jaramillo C, Urban MA, Obokhuenobe F, et al. Improving the taxonomy of fossil pollen using convolutional neural networks and superresolution microscopy. *Proc Natl Acad Sci U S A.* 2020;117(45):28496–505. <https://doi.org/10.1073/pnas.2007324117>
 130. Kasai Y, Leipe C, Saito M, Kitagawa H, Lauterbach S, Brauer A, et al. Breakthrough in purification of fossil pollen for dating of sediments by a new large-particle on-chip sorter. *Sci Adv.* 2021;7(16):eabe7327. <https://doi.org/10.1126/sciadv.abe7327>
 131. Bucher S, König P, Menzel A, Migliavacca M, Ewald J, Römermann C. Traits and climate are associated with first flowering day in herbaceous species along elevational gradients. *Ecol Evol.* 2018;8(2):1147–58. <https://doi.org/10.1002/ece3.3720>
 132. König P, Tautenhahn S, Cornelissen JH, Kattge J, Bönisch G, Römermann C. Advances in flowering phenology across the northern hemisphere are explained by functional traits. *Glob Ecol Biogeogr.* 2018;27(3):310–21. <https://doi.org/10.1111/geb.12696>
 133. Root TL, Price JT, Hall KR, Schneider SH, Rosenzweig C, Pounds JA. Fingerprints of global warming on wild animals and plants. *Nature.* 2003;421(6918):57–60. <https://doi.org/10.1038/nature01333>
 134. Bucher S, Römermann C. The timing of leaf senescence relates to flowering phenology and functional traits in 17 herbaceous species along elevational gradients. *J Ecol.* 2021;109(3):1537–48. <https://doi.org/10.1111/1365-2745.13577>
 135. Nordt B, Hensen I, Bucher S, Freiberg M, Primack RB, Stevens A-D, et al. The PhenObs initiative: A standardised protocol for monitoring phenological responses to climate change using herbaceous plant species in botanical gardens. *Funct Ecol.* 2021;35(4):821–34. <https://doi.org/10.1111/1365-2435.13747>
 136. Grossart H-P, van den Wyngaert S, Kagami M, Wurzbacher C, Cunliffe M, Rojas-Jimenez K. Fungi in aquatic ecosystems. *Nat Rev Microbiol.* 2019;17(6):339–54. <https://doi.org/10.1038/s41579-019-0175-8>
 137. Klawonn I, Dunker S, Kagami M, Grossart H-P, van den Wyngaert S. Intercomparison of two fluorescent dyes to visualize parasitic fungi (Chytridiomycota) on phytoplankton. *Microb Ecol.* 2021;1–15. <https://doi.org/10.1007/s00248-021-01893-7>
 138. Fang Y, Ramasamy RP. Current and prospective methods for plant disease detection. *Biosensors.* 2015;5(3):537–61. <https://doi.org/10.3390/bios5030537>
 139. Johansson JF, Paul LR, Finlay RD. Microbial interactions in the mycorrhizosphere and their significance for sustainable agriculture. *FEMS Microbiol Ecol.* 2004;48(1):1–13. <https://doi.org/10.1016/j.femsec.2003.11.012>
 140. Prigione V, Lingua G, Marchisio VF. Development and use of flow cytometry for detection of airborne fungi. *Appl Environ Microbiol.* 2004;70(3):1360–5. <https://doi.org/10.1128/AEM.70.3.1360-1365.2004>
 141. Liang L, Engling G, Cheng Y, Duan F, Du Z, He K. Rapid detection and quantification of fungal spores in the urban atmosphere by flow cytometry. *J Aerosol Sci.* 2013;66:179–86. <https://doi.org/10.1016/j.jaerosci.2013.08.013>
 142. Calvert MEK, Lannigan JA, Pemberton LF. Optimization of yeast cell cycle analysis and morphological characterization by multispectral imaging flow cytometry. *Cytometry A.* 2008;73A(9):825–33. <https://doi.org/10.1002/cyto.a.20609>
 143. Staley JT. Bacteria, Their Smallest Representatives and Subcellular Structures, and the Purported Precambrian Fossil “Metallogenium”. In *Microorganisms, National Research Council Steering Group for the Workshop on Size Limits of Very Small (Ed.): Size Limits of Very Small Microorganisms: Proceedings of a Workshop: National Academies Press (US).* 1999. Available from: <https://www.ncbi.nlm.nih.gov/books/NBK224752/>.
 144. Li Y, Mahjoubfar A, Chen C, Niazi KR, Pei L, Jalali B. Deep cytometry: deep learning with real-time inference in cell sorting and flow cytometry. *Sci Rep.* 2019;9(1):11088. <https://doi.org/10.1038/s41598-019-47193-6>
 145. Lee JA, Spidlen J, Boyce K, Cai J, Crosbie N, Dalphin M, et al. MIFlowCyt: the minimum information about a flow cytometry experiment. *Cytometry A.* 2008;73(10):926–30. <https://doi.org/10.1002/cyto.a.20623>
 146. Spidlen J, Breuer K, Brinkman R. Preparing a Minimum Information about a Flow Cytometry Experiment (MIFlowCyt) compliant manuscript using the International Society for Advancement of Cytometry (ISAC) FCS file repository (FlowRepository.org). *Curr Protocols Cytometry.* 2012;10(1):10.18.1–10.18.26. <https://doi.org/10.1002/0471142956.cy1018s61>
 147. Spidlen J, Novo D. ICEFormat—the image cytometry experiment format. *Cytometry A.* 2012;81(12):1015–8. <https://doi.org/10.1002/cyto.a.22212>
 148. Filby A, Davies D. Reporting imaging flow cytometry data for publication: why mask the detail? *Cytometry A.* 2012;81(8):637–42. <https://doi.org/10.1002/cyto.a.22091>

How to cite this article: Dunker S, Boyd M, Durka W, Eler S, Harpole WS, Henning S, et al. The potential of multispectral imaging flow cytometry for environmental monitoring. *Cytometry.* 2022;101(9):782–99. <https://doi.org/10.1002/cyto.a.24658>